Universidade de Aveiro
2018
Departamento de Química

Bruno Filipe Gonçalves Freitas

Desenvolvimento de Agregados de Nanopartículas contendo Fármacos para Aplicação na Medicina Regenerativa

Development of nanoparticles aggregates containing pharmaceuticals for application in regenerative medicine

Universidade de Aveiro
Ano 2018
Departamento de Química

Bruno Filipe Gonçalves Freitas

Desenvolvimento de Agregados de Nanopartículas contendo Fármacos para Aplicação na Medicina Regenerativa

Development of nanoparticles aggregates containing pharmaceuticals for application in regenerative medicine

Dissertação apresentada à Universidade de Aveiro para cumprimento dos requisitos necessários à obtenção do grau de Mestre em Biotecnologia-ramo biomolecular, realizada sob a orientação científica do Doutor Vítor Gaspar e do Professor Doutor João Mano, Professor Catedrático do Departamento de Química da Universidade de Aveiro

o júri

presidente

Professora Doutora Ivonne Delgadillo Giraldo

professor associado C/ Agregação, Universidade de Aveiro

Professora Doutora Catarina Rodrigues de Almeida

professor auxiliar em Regime Laboral, Universidade de Aveiro

Doutor Vítor Manuel Abreu Gaspar

Investigador de Pós Doutoramento, Departamento de Química da Universidade de Aveiro

Acknowledgements

First, I would like to express my thanks to Prof. Dr. João Mano for giving me the opportunity to work in his research group (COMPASS), for providing me access to all the activities that the COMPASS group participated in, from all the outstanding lectures with renown people, the international symposium, as well as for insightful discussions throughout the year.

Secondly, I thank my supervisor Dr. Vítor Gaspar for everything he teached me during the year and making sure I always had every possible tool available necessary for my success. Particularly, for devotedly presenting me with a vast possibility to learn and experience in several areas both in laboratory techniques in drug delivery technologies and cell culture. More importantly, I thank him for going beyond the supervisor's duties and extending his trust in my abilities, pushing me do much more than before in laboratory and scientific research, supporting me throughout the entire thesis. Part of what I will become in the future, better professional and, if I am to become, a good researcher it will definitely be influenced by his mentoring.

I am also grateful to all the members of the COMPASS group who have participated in helpful discussions throughout this thesis and have made the daily laboratory routine a pleasant experience. In particular my fellow Master Students that helped trough out the harshest times of this year. To my comrades and friends Luís and Pedro for all the fun and unforgettable moments and unbendable support which lead to a much healthier environment.

Lastly but not least, to all my friends since the Biochemistry's Bachelor's and in the Biotechnology Masters, as well to friends previous to the university life. Your friendship is unforgettable and helped countless times throughout the year. You have a special space in this here for their unrelenting support. I thank also all of my family, specially my Mother, Father and brother for their support and for all the sleepless nights throughout the year. This work would not be possible without their love and I profusely thank all the sacrifices they have made.

For all the experiences and knowledge accrued over this work, I thank all of those who, in some way or another, have helped me along this journey. This thesis in the end means much more, than anything other, on a personal level.

palavras-chave

Biomateriais Poliméricos, Entrega de fármacos, Nanopartículas, Géis coloidais, Aplicaçoes Biomédicas

resumo

A Inflamação crónica e doenças musculoesqueléticas são dois tipos de doenças com maior crescimento a cada ano e já atingem uma percentagem significativa da população mundial.

Os tratamentos habituais, para ambos os casos, geralmente implicam longos períodos de tempo e alto custos associados. Portanto, é de grande interesse o desenvolvimento de novos materiais que possam funcionar como sistema de entrega de fármacos a longo prazo e no local de interesse. Neste contexto, a utilização de novas abordagens farmacológicas através da utilização de produtos naturais como os flavonoides (e.g., Quercetina e Naringina) surge como uma abordagem promissora. A Quercetina é um flavonol encontrado naturalmente em muitas frutas, legumes, folhas e grãos e é descrita como contendo propriedades antioxidantes. A Naringina é uma flavona natural que ocorre naturalmente em frutas cítricas com bioatividade descrito em vários distúrbios ósseos e capaz de promover a diferenciação osteogênica de células-estaminais. No entanto, estes flavonoides são geralmente hidrofóbicos e possuem uma baixa biodisponibilidade pois são rapidamente metabolizadas *in vivo*, o que tende a limitar muito o seu uso terapêutico. O desenvolvimento de sistemas para a entrega destes fármacos de uma forma focalizada é de grande interesse no contexto de doenças que estão localizados num determinado tecido ou órgão. No entanto o desenvolvimento destas plataformas é bastante desafiante e até à data apenas pequenos avanços foram conseguidos

Neste contexto, esta tese foca o desenvolvimento de dois tipos de géis coloidais compostos por partículas poliméricas com capacidades de encapsulamento de diferentes tipos de flavonoides. Para o encapsulamento da Quercetina, um gel coloidal composto por nanopartículas aniónicas de Zeína e ácido hialurónico (150.5 ± 0.7 nm) que foram combinadas com partículas catiónicas de PLGA revestidas por poli(etilenimina) (PEI) (218.9 ± 2.7 nm). Estes sistemas apresentaram uma elevada eficiência de encapsulação de Quercetina (92 ± 1 %) através do método nanoprecipitação. A Quercetina presente no gel coloidal obteve uma libertação controlada seguindo um perfil relativamente lento de libertação em condições fisiológicas (pH = 7.4) ao longo de 20 dias. O gel foi posteriormente colocado em contato macrófagos e a sua citotoxicidade foi avaliada. A produção de NO pela indução de resposta inflamatória por LPS e sucessiva ação do gel com Quercetina foi determinada pelo método de Griess que demonstrou uma diminuição da produção de NO por parte dos macrófagos.

Por forma a melhorar as propriedades mecânicas e permitir a fixação *in situ* foram também produzidos géis coloidais com uma dupla reticulação. Para o encapsulamento de Naringina um tipo diferente de nanopartículas de Zeína ácido hialurónico metacrilado (155.9 ± 0.9 nm) foram combinadas com as partículas PLGA revestidas por poli(etilenimina) metacrilada (PEIm) (229.7 ± 1.6 nm). Este sistema demonstrou uma elevada eficiência de encapsulação Naringina (64 ± 7 %) em partículas de Zeína através do método nanoprecipitação. O perfil de libertação do gel coloidal formado por reticulação UV foi comparado com um gel coloidal formado por reticulação electroestática. Interessantemente o gel metacrilado demonstrou um perfil de libertação mais lento quando comparado com o seu antecessor. Posteriormente para avaliar a atividade pró-osteogénica deste sistema o gel foi colocado em contato com células-estaminais de tecido adiposo humano (ASCs). Os resultados obtidos demonstraram que o sistema coloidal reticulado por UV induz uma maior expressão da enzima alcalina fosfatase quando comparado com o meio pro-osteogénico ou a administração de Naringina na sua forma livre. No geral, os géis coloidais de dupla reticulação apresentam-se como uma promissora plataforma para entrega local de flavonoides e demonstraram potencial para futuras aplicação como sistemas moldáveis aos diferentes tipos de danos tecidulares.

keywords Biomedical Applications, colloidal Gels, Drug delivery, Nanoparticles, Polymeric biomaterials

abstract

Chronic Inflammation and Musculoskeletal Diseases are two types of diseases with greater growth each year and already reaching a larger portions pf the population worldwide.

The usual treatments, for both cases, are usually implicated in large periods of time and high associated costs. Therefore, the development of new materials that can be performed as a focal long-term drug delivery system is of great interest. In this context, the use of new pharmacological drugs through the use of natural products such as flavonoids (eg Quercetin and Naringin) appear as a promising approach. Quercetin is a flavonol naturally found in many fruits, legumes, leaves and granules and is exposed to antioxidant properties. Naringin is a naturally occurring flavone that occurs naturally in citrus fruits with bioactive in various bone disorders and may have promising in the boundary osteogenesis of stem cells. However, these flavonoids are typically hydrophobic and have low bioavailability because they are rapidly metabolized in vivo, which may limit their therapeutic use. The development of systems for drug delivery in a focused way is of great interest for a different plan of action. However the result of the operations is quite challenging and even the data are only visible were achieved

In this context, this thesis focus on the development of two types of colloidal gels component compose of polymeric particles with efficient encapsulation of different types of flavonoids. For the encapsulation of Quercetin, a colloidal gel composed of anionic nanoparticles of Zein and hyaluronic acid (150.5 ± 0.7 nm) that were combine with PLGA coated in poly (ethylene) (PEI) as cationic nanoparticles (218.9 ± 2, 7 nm). These system present a high efficiency of Quercetin encapsulation (92 ± 1%) through the nanoprecipitation method. The Quercetin present in the colloidal gel had a controlled drug release profile relatively slow under physiological (pH =7 4) for the period of 20 days. The gel was afterwards put in macrophagic contact and its cytotoxicity was evaluated. The production of NO by the induction of inflammatory response by LPS and successive action of the gel with Quercetin was determined by the Method of Griess demonstrating a production of NO by macrophages.

In order to improve the mechanical properties and to allow *in situ* fixation colloidal gels with a double crosslinking were also produced. The encapsulation of Naringin is a type of Zein nanoparticles methacrylated hyaluronic acid (155.9 ± 0.9 nm) with combinations of PLGA nanoparticles coated with poly (ethylenimine) methacrylate (PEIm) (229.7 ± 1.6 nm). This system demonstrated maximum efficiency of Naringin encapsulation (64 ± 7%) in Zein particles through the nanoprecipitation method. The release profile of the colloidal gel formed by UV crosslinking was compared to a colloidal gel formed by electrostatic crosslinking. Interestingly the methacrylated gel showed a slower release profile when compared to its predecessor. Subsequently for a pro-osteogenic consultation of this system the gel was placed in contact with human adipose tissue stem cells (ASCs). The results obtained demonstrate that the UV-crosslinked colloidal system has a greater expression of the enzyme alkaline phosphatase when compared to the pro-osteogenic or administration of enzymes in their free form. In general, double-crosslinked colloidal gels are a promising platform for the local delivery of flavonoids and demonstrate potential for the application of intelligent systems to different types of tissue damage.

Contents

List of Figures

List of tables

List of abbreviations and Acronyms

4NPh	4-Nitrophenol 10 mM
4NPhP	4-Nitrophenyl phosphate disodium salt hexahydrate
AA	L-ascorbic acid 2-phosphate magnesium salt
ASCs	Human adipose stem cells
BG	β-glycerophosphate disodium salt hydrate
DEA	Diethanolamine
Dex	Dexamethasone
DiD	Vybrant™ DiD Cell-Labeling Solution
DiO	Vybrant™ DiO Cell-Labeling Solution
DLS	Dynamic light scattering
DMEM	Dulbecco's Modified Eagle Medium
EDC	1-(3-Dimethylaminopropyl)-3-ethylcarbodiimide
FBS	Fetal Bovine Serum
Gel-Nar	Naringin in colloidal gel
Gel-Q	Quercetin in colloidal
GM	Glycidyl methacrylate
HA	Hyaluronic Acid
HAm	Hyaluronic Acid methacrylate
Irgacure	Hydroxy-4'-(2-hydroxyethoxy)-2-methylpropiophenone
LPS	LPS from *E. coli* EH100 (Ra) TLR pure Sterile Son
MA	Methacrylic acid
ML	Mass loss
Nar	Naringin
NHS	N-Hydroxysuccinimide
NO	Nitric oxide
NP	Nanoparticle
OM	Osteogenic differentiation medium
PBS	Phosphate buffered saline (PBS, 10x)

PDI	Size distribution
PDMS	PDMS - Dow Corning 184 Silicone Elastomer Kit
PEI	poly(ethyleneimine)
PEIm	Poly(ethyleneimine) methacrylate
PLGA	Poly(D,L-lactide-co-glycolide)
PLGA-PEI NPs	PLGA-PEI conjugate nanoparticles
PLGA-PEIm NPs	PLGA-PEIm conjugate nanoparticles
PVA	Polyvinyl Alcohol
STEM	Scanning Transmission Electron Microscopy
SW	Swelling
Trehalose	D-(+)-Trehalose Dihydrate (2H2O)
UV-Vis	Ultraviolet-visible
WC	Water content
Zein-HA NPs	Zein hyaluronic acid crosslinked nanoparticles
Zein-HAm NPs	Zein hyaluronic methcarylate acid crosslinked nanoparticles
αMEM	α-MEM powder (-nucleosides, +L-glutamine)

List of publications

I Review article: “Self-assembled Colloidal gels for diverse biomedical applications – Advances and prospects”. Manuscript under preparation.

II Article: “Multicomponent Self-assembled Colloidal Gel for Focal Drug delivery”. Manuscript under preparation.

III Article: “*In situ* photocrosslinkable double-network colloidal gel as injectable bioactive depots for tissue engineering”. Manuscript under preparation.

1.Introduction

1.1. Self-assembled Colloidal gels for diverse biomedical applications – Advances and prospects

Subchapter 1.1.

This subchapter is based on the article entitled

"*Self-assembled Colloidal gels for diverse biomedical applications – Advances and prospects*"

Self-assembled Colloidal gels for diverse biomedical applications – Advances and prospects

Bruno Freitas, Vítor M. Gaspar[#] and João F. Mano[#]

Department of Chemistry, CICECO – Aveiro Institute of Materials, University of Aveiro, Campus Universitário de Santiago, 3810-193, Aveiro, Portugal.

[#]Corresponding authors:
Professor Dr. João F. Mano
Department of Chemistry, CICECO – Aveiro Institute of Materials
University of Aveiro, Campus Universitário de Santiago
3810-193, Aveiro, Portugal
E-mail: jmano@ua.pt
Telephone: +351 234370733
Dr. Vítor Gaspar
Department of Chemistry, CICECO – Aveiro Institute of Materials
University of Aveiro, Campus Universitário de Santiago
3810-193, Aveiro, Portugal
E-mail: vm.gaspar@ua.pt
Telephone: +351 234370733

Abstract

Colloidal gels are a class of biomaterials comprise of a continuous network of assembled particles in an arrested state that can yield multifunctional materials with tunable mechanical properties. The building block of the colloidal gel, the nanoparticles, serve as mechanical nanostructures and, as well, as drug deposits for drug delivery if required. The mechanical properties of these gels also depend greatly from the particle composition, inorganic or organic. The network achieve in colloidal gels is denser than those seen in hydrogels and alike differing greatly from these systems. Also, the diffusion from the surrounding medium to the interior of the colloidal can occur trough the porous network presented in colloidal gels and not depending on the mass barriers of hydrogels.

These review aims to show the colloidal interactions of different particle composition and showcase the biomedical application of the best materials in both inorganic and organic domains.

1. Introduction

In the past years, the demand for novel tissue engineering platforms and new medical strategies in regenerative medicine have increased exponentially. This demand led to the rapid development of platforms such as hydrogels, a well-established technology in biomaterial sciences nowadays.[1] By no means outdated and still very versatile, the hydrogel is a versatile platform that can allow cell adhesion and mimic native tissue to a certain degree. However, current hydrogel applications lack drug delivery potential due to lack of true controlled sustained release from the aqueous 3D polymeric network.[2] One way to approach this problematic is to embed nano- or microparticles within the hydrogels frameworks, therefore allowing a more tailored release profile from the hierarchic system established in terms of particle matrix, hydrogel structure and surrounding microenvironment. Moreover, improved mechanical robustness and further sustained bioactive molecules release can be obtained by using the particles as focal crosslinking points within the hydrogel network. Unfortunately, such hybrid systems require that the crosslinking mechanisms must be adapted for each case, in lieu of compromising the integrity and porosity of the polymeric structure, thus completely changing the release profile of the platform.[3]

So in most recent years, the necessity to develop complex and localizable drug releasing systems is not being fully met through hydrogel platforms. Improving upon the current hydrogel design may lead to the development of sophisticated tissue engineering platforms and biomaterials with tailored conditions. Some of such conditions are the capability to adequately support cell growth in hydrated 3D environments with easy diffusion of nutrients and various chemokines, as well as the adaptability to be implanted in patients and correctly fit into defects. Also, mimicking the living tissue is important for optimal regenerative properties and even so to deliver pharmaceuticals with temporal and spatial control.[4] Thus, in the search for novel platforms, a new approach is currently being exploited, namely colloidal gels, that are dense structures formed from individual particles organized in bulk porous structures.[5] These bulk porous structures allow for nutrients and other bioactive compounds to flow freely throughout the network of a colloidal gel and still have a drug delivery mechanism implemented, something not quite possible in typical hydrogels. However, currently developed colloidal gel structures are hindered by weak temporary electrostatic, Van der Waals or hydrophilic/hydrophobic interactions between particles while

dispersed in liquid, which limits their stability and mechanical properties.[6,7,8] Still, in this review we will show more approaches regarding colloidal assembly. However, as mentioned before, due to the nature of these transient electrostatic interactions, the mechanical properties of the majority of current colloidal gels far from desired.[6] The bulk structure inherent to colloidal gels provides a tunable mechanical property, because different particles species can be included within these systems.[4] Such flexible character brings several advantages for the nanostructure properties in terms of viscoelasticity, injectability, cohesiveness recovery and in vitro degradation.[4] Also these characteristics have been further studied in rheological models establishing the shear-thinning properties of colloidal gels in the form of changes in viscosity, as well as the possibility to tailor the water content, that also plays a key role in the resulting mechanical properties.[4]

So the method of fabrication from particles to macro structures, Top-down approach, also presents many advantages to regular biomaterials. The resulting mesoporous platform can achieve an even increased complexity compare to regular biomaterials. Both in composition and structure of particles can be tune down and combined sustain drug delivery and cellular and tissue engineering.[9] The use of particles similar as building blocks is an benefit in drug delivery systems and tissue engineering applications due to the general sustained release profile of then, if intended as such.[10,11] The release kinetics by the particle structure overcome most issues in mass transport barriers characteristic of hydrogels. However particle size can affect loading and release profile of drugs, fortunately most particles have change in size depending of its formulation, design and method of fabrication.[10,2] As in colloidal gels, the size becomes more as to nanoparticles benefit of having higher surface energy compared to microparticles, while the drug loading decrease and drug release increase as the dimensions of the particle decreases. The nanoparticle have a more chemically reactive surface and higher affinity to bind and interact with materials which is specially captivating for colloidal gels.[12,4] Furthermore, for a colloidal gel the particle must also have in consideration its purpose as it influences the bioavailability and interaction to the surrounding medium. As designing organic and inorganic particles alike, this when made enough large depending of the type of particle, can be captured by systems as the reticuloendothelial system which leads to more rapid degradation than sometimes is intended.[13] Also, for drug release profile size is a significant factor as microparticles tend to have larger release profiles than nanoparticles,

however when larger than 25 μm might promote inflammation response. For both microparticles and nanoparticles, usually, have a more extent drug release than hydrogels.[14]

As colloidal gels, formulations tend to prefer higher surface charges increase electrostatic interactions, as it will be shown further. Also, different release profiles can be created from combining different particles quantities and species when manufacturing the colloidal gel.[15] In this review, we intend to highlight the most recent promising and relevant colloidal gel systems developed so far as well as its applications. Although electrostatic interactions are the main driving forces in colloidal gels, some studies use external or internal stimuli to change how the inter-particle interactions occur, an alternative design methodology that will also be briefly touch upon throughout this review.

2. Nature of particles that build a colloidal gel

As said formerly, a colloidal gel is a cluster of particles, usually nanoparticles (NP). NPs are typically use due to higher surface charge, but also due to specific advantages and versatility. As such, being capable of release therapeutic agents in a control manner either from extracellular or intracellular environment, cause by their easier internalization compare to microparticles. These higher internalization can also be exploit for the area of targeted imaging, even while co-delivering in system.[16] Furthermore, these subdivisions of the gel, NPs, typically form from different approaches of fabrication. Methods such emulsion, nanoprecipitation and dispersion polymerization are widely use and process most kind of NPs. To construct the particle the procedure use the physicochemical properties such as electrostatic, hydrophilic/hydrophobic and physical or chemical crosslinks.[17] Furthermore, the application of the particles into colloidal gels form must have in its design certain characteristics such as mechanical support, a bioactive role, drug delivery or cell targeting.[18] For the many roles a colloidal gel can be presented itself, a central characteristic in his costituent NPs. The NP must have a ell define core structure and a surface with the intended charge and/or functional groups. The core of the particle usually forms from a solid core or a polymeric one which define some of the attributes of the particle as size, drug loading and delivery and also the its mechanical properties.[19] The surface outlines the particle, the charge of it, gives the particle cell adhesion or cell targeting and is the fundament of colloid interaction between particles.[18]

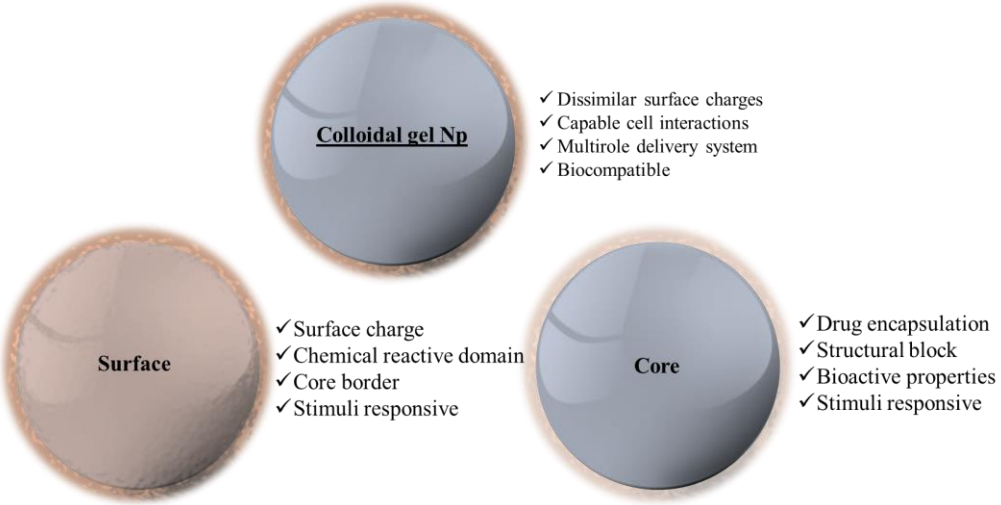

Figure 1. Nanoparticle properties for colloidal gel formulation. A colloidal gels require a set a properties in the NPs which can lead to complex formulations, these formulations

pursue to influence both the core and surface charge have their importance. Although most of the time are the same material, the core contributes most as a mechanical asset or a drug carrier depending of the material choose. The NP surface mostly contributes to the cohesive property in the colloidal gel, while sometimes retain reactive groups for extra applicability. Further on it will be shown the difference in NP in the core sets with different applications and the surface effect and its applications.

To achieve the polymeric entanglement it is required one of two different mechanisms, this being covalent cross-link and non-covalent cross-link. Both mechanisms use, in different ways, Van der Waals, electrostatic and hydrophilic/hydrophobic interactions to enable such self-assemble structure. In association, the procedures applied to produce well shape and controlled size particles explore this such properties. Techniques as emulsion, nanoprecipitation, microfluidic and many other methods are further explain in others reviews and generally all produce particle with well define size.[20,21,22] Like so, the same interactions properties of the polymeric material also allows for the encapsulation of bioactive compounds within its polymeric matrix.[23] In result, the use of such techniques depend mostly on the polymer use, some polymers like the synthetic ones like PLGA [24,5,25,2], PEG [4,26], and others [27,28] are already being use in the formulation of colloidal gels. Likewise, it is use natural origin polymers as self-assembly polysaccharide particles and functionalize polysaccharides in specific particle formulations. Also, protein derive particles are use as due to interesting properties shown in forth. While synthetic polymers tend to acquire a more plastic or micellar kind of particles, natural polymers as polysaccharides make use of the monomers and its reactive groups. Dynamic bonding's, hydrogen bonds or metal complexation are only a few of the multiple interaction's polymers such as alginate, hyaluronic acid, chitosan, amylose, cellulose and many others are capable. Furthermore, functionalize polysaccharides increase even further the versatility of natural occurring polymers. Functional groups added to the chain of polymer can serve as additional cross-linking point by mechanism as host guest, electrostatic hydrophobic or metal complexation not present beforehand.[23] Thus, by addition of tailor-made specific sensitive groups into the polymer chain the self-assembly nanogels can acquire stimuli responsive behaviours. Chemical groups such as carboxylic acid, amine and thiol usually are the reason of most of the internal stimuli as NP can sense. Such internal stimuli are pH, redox potential, ionic strength, temperature responsive, enzymatic and specific trigger such as glucose present in Mónica C. García et. al. 2018.[17] Unlike, the first three responsive stimuli temperature,

enzymatic and specific compounds trigger are not directly dependent of the chemical groups and often depend of physical crosslinks[29], hydrophilic/hydrophobic synergy[30] and non-physiological radical crosslinks[31] respectively. External stimuli such as light, ultrasound and magnetic field have gain remarkable attention in recent years mainly due to the non-invasive remote step when apply under physiological conditions and with compound drug delivery systems. The array of trigger stimuli response is further explain in figure.2 and showcase some [17]

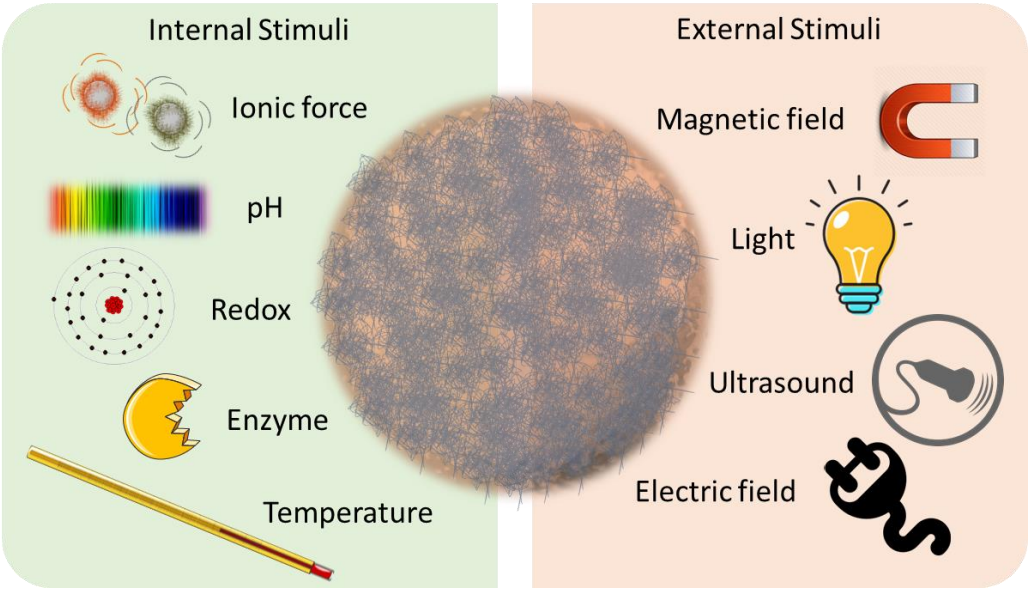

Figure 2. Different internal and external stimuli responses in nanoparticles. In ionic response it mostly occurs trough the competition of bioactive compound to other ions for the interaction to the polymeric matrix. In pH response slight changes in pH, for example from 7.4 plasma values to 6.5 pH in tumour medium, or 4-5 in lysosomes intracellular organelle, allows the change in charges across the polymer modifying the interaction of the drug to the 3D microenvironment granting a framework for new drug delivery platforms. In redox response the mechanisms employed make use of the natural body reduction potential, usually glutathione levels, the nanogels mainly are functionalize with -thiol groups that respond to alterations in the reductive potential in the medium. In enzyme response the use of peptide sequences in the polymer frame or the polymer itself to enzyme recognition, for example hyaluronic/ hyaluronidases. In temperature response polymers with low critical solution temperature as a property.[32] A in external stimuli, unlike ultrasound which can be use in polymer base NP and hydrogels for drug delivery. Usually these stimuli requires metal compounds as metal nanoparticles as iron oxide NP for magnetic field, Gold nanorods for light response, or any conductor for electric field in biosensors. It's worth mentioning that some organic compounds react to light in a control manner as such spiropyran[33], azobenzene[34] and polydopamine NP[35]. Adapted from reference [17].

The factors responsible for the stimuli response do so by changing the internal microenvironmental of the nanogel forcing an rearrangement of the 3D polymeric structure and/or an conformational arrangement, this leading to a different release profile of bioactive compound.[17] In this context, this chapter aims to cover which type of NP is use in the formation of most recent and significant colloidal gel platforms and its applications. We will highlight composition, resolution and impact on the characteristics of colloidal gel form from a NP perspective.

2.1. Organic particle

Polymeric particles, or like some papers present, a nanogels have an increase attention in last years in tissue engineering, drug delivery, and biomaterials fields due to several capabilities. In terms of applicability synthetic polymers like PLGA, PEG, but also Latex are already being use in the formulation of colloidal gels. Their main advantage compared to other polymers is the natural highly controlled degradation profile. As an example PLGA a aliphatic polyester copolymer, one of the main polymer use in colloidal gels, is a combination of D,L-Lactide acid and Glycolide acid and the ratio between both in the degradation profile is well documented being the most degradable 50:50 ratio and the less degradable 85:15, Lactide:Glycolide.[36] Also PLGA is a versatile and easily tunable polymer with good mechanical behaviour, which can be processed into any shape and size. In the work of *Qun Wang* et. al, 2008 the researchers use simple cationic and anionic PLGA nanoparticles made by the method of nanoprecipitation, the electrostatic force between particles is enough acquire a pseudoplastic behaviour to hold intricate forms as show in fig. 3.

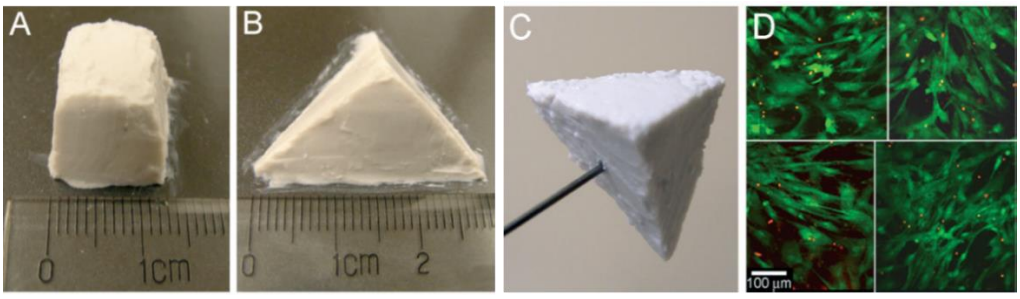

Figure 3. The colloidal gel form from PLGA nanoparticles has enough mechanical strength to hold different geometric forces, square (A) and pyramid (B) and its able to be handled in a tip of a needle (C). Also, human umbilical cord matrix stem cells seeded on the

top of the colloidal gel have large cell adhesion as seen and have minimal cell death (D). Adapted from reference [37].

It is also noteworthy, this colloidal gel under SEM observation show perfectly the natural bulk porous structure of the colloidal gel, fig. 4.

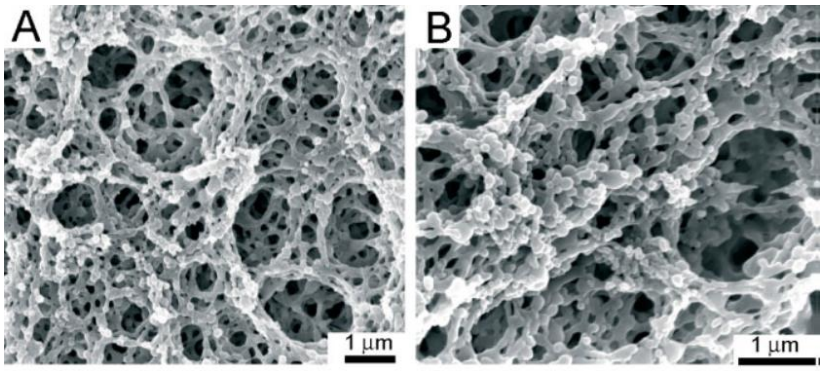

Figure 4. The Sem image reveals porous of a few micrometres, largely compared to the size of the particle, around 185 nm. Adapted from reference [37].

However, colloidal gels due to the top down fabrication denoted previously can make use of interesting approaches such as in the work of Yue Zhang et. al. 2017. The researches focused on obtaining a compelling biomimetic system by combining PLGA with chitosan into a cationic nanoparticle with a anionic PLGA nanosponge coated in Red Blood cell membrane (RBC). The network obtain has the normal mechanical properties of a colloidal gel, self-healing capability and other properties as show in fig. 5.[10]

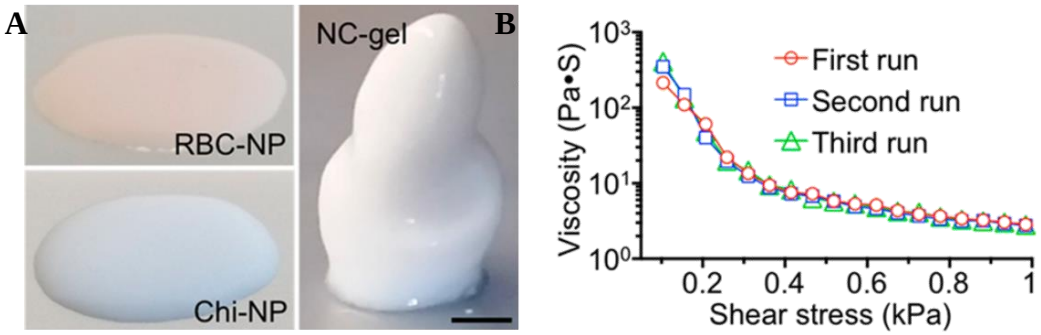

Figure 5. Standing alone each NP presents very little viscosity, however when combine the electrostatic force from both particles creates an increased resistance forming a colloidal gel (A). Further on the viscosity is confirm in rheological experiments (B). Adapted from reference [10].

However, the best result of this colloidal gel is grant to the clever design of the anionic particle, first the fabrication of the particle uses a simple process as sonication to produce

PLGA-RBC NP. This method allows a biofunctionalise particle with inherent tuned physicochemical properties of the PLGA and a display of the natural surface antigens of RBC. Thus, retaining the full capacity to inhibit toxin-induced hemolysis even in colloidal gel form.[10]

2.2. Inorganic particle

Traditionally, inorganic nanoparticles are already incorporate into hydrogel matrix for improve mechanical properties.[38] With the use of nanoparticles as crosslinkers in hydrogels trough specific interactions the bonds result in a polymeric network with greater elasticity as nanoparticles presents its natural properties. And so, some researchers start to notice the possibility of using inorganic nanoparticles as a matrix all by itself, an colloidal gel by all means. These is also cause by components of hybrid systems achieve unique physicochemical and biological properties, however colloidal gels alone accomplish biointerfacing properties attractive to many medical issues.[2] The type of inorganic nanoparticle allows the colloidal gels different possible interactions to cells and these interactions can increase or decrease the activity of cells, provide a mechanism of defence or simple serve as a filler material with desirable characteristics in a colloidal gel as it will be shown further.[39]

One inorganic NP is very interesting to use as a building block in colloidal gels, especially in bone regeneration, hydroxyapatite NP is a inorganic particle with a bioresorbable property, meaning after a certain time its starts to break apart and is capable of being absorbed by the body and be use if so to supply minerals for newly form bone tissue. And so, researchers like Qun Wang et. al. 2013 prepared a colloidal gel of cationic PLGA NP and hydroxyapatite NP. Although unfortunately no drug as encapsulate in PLGA NP for a possible synergetic osteogenic potential by the colloidal gel. Their aim of work was to achieve a colloidal gel with good mechanical properties, however the result was a dense structure which had limited cohesiveness quickly demonstrated in their process of rheological studies. Although seemingly a limitation in the next work shown the cohesiveness is not a issue as it allows for other process to occur that were not explore in this work.[40]

Following the same approach to bone regeneration, one of the most well research inorganic particle in tissue engineering is silica nanoparticles, composed mainly of

covalently bonded silica it has several different procedures of manufacture. Yet, most recent procedures form NPs at room temperature. This process allow the same physicochemical property encountered previously while being capable of biofunctionalise the NP without thermal degradation inherent of previous process. The low toxicity, tissue attachment and possible ion exchange platform makes this NPs very desired in tissue engineering, mainly osteoporotic approaches. Implants made from this material have several advantages and can prevent the use of autologous or donor bone in bone grafting. Also, the degradation of the material is of much desire, under simulated physiological conditions such as phosphate buffered saline or culture media ionic dissociation of the material occurs which contributes positively to the activation of certain genes directly link to osteogenesis.[41] As shown in the research article of Mani Diba et.al, 2017, the use of Silica NP, bioactive glass and bisphosphonate gelatin coated NP, its combine the best of mechanical robustness with greatly osteogenic potential, both factor contribute to the bone regeneration. The propose objective in this work is to have an injectable platform for correcting of bone defects as shown in fig. 6.[39]

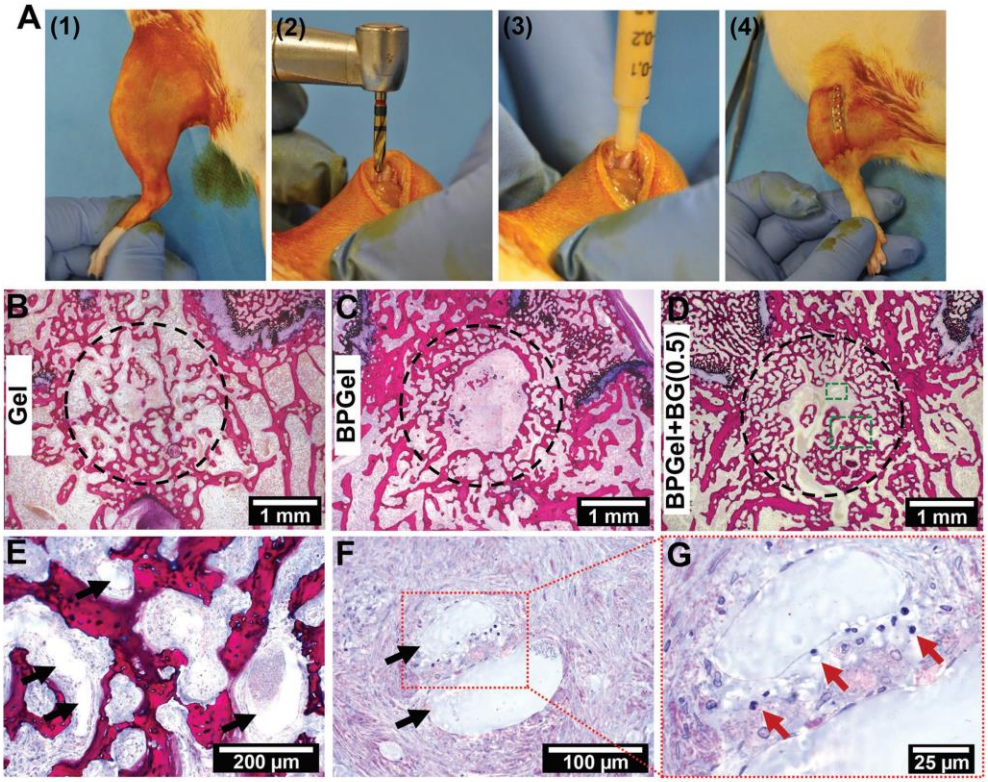

Figure 6. In vivo inorganic colloidal gel assay. In order to test the action of colloidal gel in vivo rats had a surgical procedure made to simulate a bone defect were the colloidal gel is introduced (A). Different conditions in terms of the colloidal gel composition is

tested, although all seen to have formation of vascularized bone inside (B), (C) and (D). In condition (D) the complete composition of the gel is tested, a slight increase angiogenic effect can be attributed to BG particles in and the presence of cells in the defect area (red arrows) can be due to the mechanical properties that allow cell proliferation in the gels. Retrieved from [39].

Also in this work the researches strive to achieve an enhance bond between gelatin and bioactive glass through the use of bisphosphonate groups.[39] The self-healing capability reported allowed the recovery meaning that given enough time, cells from the surrounding can start to invade the bulk porous structure. Which occurred as shown in fig. 6, proving that a more dense or stiff structure does not grant better properties, as cohesiveness if properly plan enables a quicker regeneration of the damage area.

3. Conclusion

In summary, colloidal gels are continuous networks of arrested particles due to interactions established among themselves. Although electrostatic interactions account for most of the colloidal network assembly, it is worth noting that some other interactions may drive the colloidal gelation process, such as those induced by temperature[42,43], pH [6], catechol conjugation chemistries [38] and protein-mediated assemblies[28]. An alternative way for formulating novel colloidal gels would be the use of Janus particles, as recently demonstrated by Joshua Avossa *et. al*. 2018, which could net interesting colloidal gels due to opposing charges in each silica particle's opposing poles. Colloidal gels assembled from an unique particle species containing different surface charges depending on the location within the particle could yield new physicochemical properties from the resulting colloidal gel network. [45]

Other applications of colloidal can be the use of them as inverse colloidal systems, in which the particles form the colloidal gel and act as a template for building a porous structure containing the exact dimensions and surface morphology of the colloidal framework removed.[46] Also, colloidal gels are slowly making their way to bioprinting applications, even though some issues such as gel breakdown due to extrusion will need be overcome by designing advanced colloidal gel systems beyond those simply electrostatically-driven assemblies. [47]

As showcased earlier, colloidal gels have immense potential and multiple possible applications that are not limited to only biomedical applications but also be applied in several other research areas, namely ink manufacturing, electronics and metal colloids.

4. References

1. Jiang, Y., Chen, J., Deng, C., Suuronen, E. J. & Zhong, Z. Click hydrogels, microgels and nanogels: Emerging platforms for drug delivery and tissue engineering. *Biomaterials* **35,** 4969–4985 (2014).

2. Gao, W., Zhang, Y., Zhang, Q. & Zhang, L. Nanoparticle-Hydrogel: A Hybrid Biomaterial System for Localized Drug Delivery. *Ann. Biomed. Eng.* **44,** 2049–2061 (2016).

3. Shen, Y., Nyström, G. & Mezzenga, R. Amyloid Fibrils form Hybrid Colloidal Gels and Aerogels with Dispersed CaCO3 Nanoparticles. *Adv. Funct. Mater.* **27,** 1–9 (2017).

4. Roux, R., Ladavière, C., Montembault, A. & Delair, T. Particle assemblies: Toward new tools for regenerative medicine. *Mater. Sci. Eng. C* **33,** 997–1007 (2013).

5. Wang, Q., Wang, L., Detamore, M. S. & Berkland, C. Biodegradable colloidal gels as moldable tissue engineering scaffolds. *Adv. Mater.* **20,** 236–239 (2008).

6. Diba, M., Wang, H., Kodger, T. E., Parsa, S. & Leeuwenburgh, S. C. G. Highly Elastic and Self-Healing Composite Colloidal Gels. *Adv. Mater.* **29,** (2017).

7. Wang, Q., Gu, Z., Jamal, S., Detamore, M. S. & Berkland, C. Hybrid Hydroxyapatite Nanoparticle Colloidal Gels are Injectable Fillers for Bone Tissue Engineering. *Tissue Eng. Part A* **19,** 2586–2593 (2013).

8. Wang, H. *et al.* Combined delivery of BMP-2 and bFGF from nanostructured colloidal gelatin gels and its effect on bone regeneration in vivo. *J. Control. Release* **166,** 172–181 (2013).

9. Wang, H. *et al.* Development of injectable organic/inorganic colloidal composite gels made of self-assembling gelatin nanospheres and calcium phosphate nanocrystals. *Acta Biomater.* **10,** 508–519 (2014).

10. Zhang, Y. *et al.* Self-Assembled Colloidal Gel Using Cell Membrane-Coated Nanosponges as Building Blocks. *ACS Nano* **11,** 11923–11930 (2017).

11. Park, J., Kim, S. & Kim, K. Bone morphogenetic protein-2 associated multiple growth factor delivery for bone tissue regeneration. *J. Pharm. Investig.* **48,** 0 (2018).

12. Dennis, S. C., Whitlow, J., Detamore, M. S., Kieweg, S. L. & Berkland, C. J. Hyaluronic-Acid–Hydroxyapatite Colloidal Gels Combined with Micronized Native ECM as Potential Bone Defect Fillers. *Langmuir* **33,** 206–218 (2017).

13. Hu, Q., Chen, Q. & Gu, Z. Advances in transformable drug delivery systems. *Biomaterials* 1–13 (2018). doi:10.1016/j.biomaterials.2018.03.056

14. Maudens, P., Jordan, O. & Allémann, E. Recent advances in intra-articular drug delivery systems for osteoarthritis therapy. *Drug Discov. Today* **23,** 1761–1775 (2018).

15. Mealy, J. E. *et al.* Injectable Granular Hydrogels with Multifunctional Properties for Biomedical Applications. *Adv. Mater.* **30,** 1–7 (2018).

16. Mano, J. F. & Reis, R. L. From nano-to macro-scale : Nanotechnology approaches for spatially controlled delivery of bioactive factors for bone ... R eview From nano- to macro-scale : nanotechnology approaches for spatially controlled delivery of bioactive factors for bone and cart. **7,** 1045–1066 (2016).

17. García, M. C. & Cuggino, J. C. *Stimulus-responsive nanogels for drug delivery*. *Stimuli Responsive Polymeric Nanocarriers for Drug Delivery Applications, Volume 1* (Elsevier Ltd., 2018). doi:10.1016/B978-0-08-101997-9.00016-3

18. Press, D. Effective use of nanocarriers as drug delivery systems for the treatment of selected tumors. 7291–7309 (2017).

19. Pfeiffer, C. *et al.* Interaction of colloidal nanoparticles with their local environment : the (ionic) nanoenvironment around nanoparticles is different from bulk and determines the physico-chemical properties of the nanoparticles. (2014).

20. Oh, J. K., Drumright, R., Siegwart, D. J. & Matyjaszewski, K. The development of microgels/nanogels for drug delivery applications. *Prog. Polym. Sci.* **33,** 448–477 (2008).

21. Kabanov, A. V. & Vinogradov, S. V. Nanogels as pharmaceutical carriers: Finite networks of infinite capabilities. *Angew. Chemie - Int. Ed.* **48,** 5418–5429 (2009).

22. Nayak, S. & Andrew Lyon, L. Soft nanotechnology with soft nanoparticles. *Angew. Chemie - Int. Ed.* **44,** 7686–7708 (2005).

23. Hashimoto, Y., Mukai, S., Sasaki, Y. & Akiyoshi, K. Nanogel Tectonics for Tissue Engineering : Protein Delivery Systems with Nanogel Chaperones. **1800729,** 1–14 (2018).

24. Wang, Q., Jamal, S., Detamore, M. S. & Berkland, C. PLGA-chitosan/PLGA-alginate nanoparticle blends as biodegradable colloidal gels for seeding human umbilical cord mesenchymal stem cells. *J. Biomed. Mater. Res. - Part A* **96 A,** 520–527 (2011).

25. Wang, Q., Wang, J., Lu, Q., Detamore, M. S. & Berkland, C. Injectable PLGA based colloidal gels for zero-order dexamethasone release in cranial defects. *Biomaterials* **31,** 4980–4986 (2010).

26. Cui, S., Yu, L. & Ding, J. Semi-bald Micelles and Corresponding Percolated Micelle Networks of Thermogels. *Macromolecules* **51,** acs.macromol.8b01014 (2018).

27. Desire, C., Lotierzo, A., Arrua, R. D., Hilder, E. F. & Bon, S. A. F. Robust Open Cellular Porous Polymer Monoliths made from Cured Colloidal Gels of Latex Particles. *Green Chem.* advance article (2018). doi:10.1039/C8GC01055B

28. Obana, M., Silverman, B. R. & Tirrell, D. A. Protein-Mediated Colloidal Assembly. *J. Am. Chem. Soc.* **139,** 14251–14256 (2017).

29. Fan, C. & Wang, D. A. Novel Gelatin-based Nano-gels with Coordination-induced Drug Loading for Intracellular Delivery. *J. Mater. Sci. Technol.* **32,** 840–844 (2016).

30. Wang, Y. *et al.* An Enzyme-Responsive Nanogel Carrier Based on PAMAM Dendrimers for Drug Delivery. *ACS Appl. Mater. Interfaces* **8,** 19899–19906 (2016).

31. Manuscript, A. Polymer Chemistry. (2013). doi:10.1039/C3PY01202F

32. Jiang, L. *et al.* PH/temperature sensitive magnetic nanogels conjugated with Cy5.5-labled lactoferrin for MR and fluorescence imaging of glioma in rats. *Biomaterials* **34,** 7418–7428 (2013).

33. Son, S., Shin, E. & Kim, B. S. Light-responsive micelles of spiropyran initiated hyperbranched polyglycerol for smart drug delivery. *Biomacromolecules* **15,** 628–634 (2014).

34. Rastogi, S. K. *et al.* Enhanced Release of Molecules upon Ultraviolet (UV) Light Irradiation from Photoresponsive Hydrogels Prepared from Bifunctional Azobenzene and Four-Arm Poly(ethylene glycol). *ACS Appl. Mater. Interfaces* acsami.6b16183 (2017). doi:10.1021/acsami.6b16183

35. Wang, X. *et al.* A Polydopamine Nanoparticle-Knotted Poly(ethylene glycol) Hydrogel for On-Demand Drug Delivery and Chemo-photothermal Therapy. *Chem. Mater.* **29,** 1370–1376 (2017).

36. Martins, C., Sousa, F., Araújo, F. & Sarmento, B. Functionalizing PLGA and PLGA Derivatives for Drug Delivery and Tissue Regeneration Applications. **1701035,** 1–24 (2017).

37. Wang, B. Q., Wang, L., Detamore, M. S. & Berkland, C. Biodegradable Colloidal Gels as Moldable Tissue Engineering Scaffolds **. 236–239 (2008). doi:10.1002/adma.200702099

38. Li, Q., Barrett, D. G., Messersmith, P. B. & Holten-Andersen, N. Controlling hydrogel mechanics via bio-inspired polymer-nanoparticle bond dynamics. *ACS Nano* **10,** 1317–1324 (2016).

39. Diba, M. *et al.* Composite Colloidal Gels Made of Bisphosphonate-Functionalized Gelatin and Bioactive Glass Particles for Regeneration of Osteoporotic Bone Defects. *Adv. Funct. Mater.* **27,** 1–12 (2017).

40. Wang, Q., Gu, Z., Jamal, S., Detamore, M. S. & Berkland, C. Hybrid Hydroxyapatite Nanoparticle Colloidal Gels are Injectable Fillers for Bone Tissue Engineering. **19,** 2586–2593 (2013).

41. Baino, F., Fiume, E., Miola, M. & Verné, E. Bioactive sol-gel glasses: Processing, properties, and applications. *Int. J. Appl. Ceram. Technol.* 841–860 (2018). doi:10.1111/ijac.12873

42. Hsiao, M. H. *et al.* A temperature-induced and shear-reversible assembly of latanoprost-loaded amphiphilic chitosan colloids: Characterization and in vivo glaucoma treatment. *Acta Biomater.* **10,** 3188–3196 (2014).

43. Salamończyk, M. *et al.* Structure of nanoscale-pitch helical phases: blue phase and twist-bend nematic phase resolved by resonant soft X-ray scattering. **4,** 962–972 (2017).

44. Fakhari, A., Phan, Q. & Berkland, C. Hyaluronic acid colloidal gels as self-assembling elastic biomaterials. *J. Biomed. Mater. Res. - Part B Appl. Biomater.* **102,** 612–618 (2014).

45. Avossa, J. *et al.* Applied Surface Science Forming nanostructured surfaces through Janus colloidal silica particles with nanowrinkles : A new strategy to superhydrophobicity. *Appl. Surf. Sci.* **465,** 73–81 (2019).

46. Kuo, Y. C. & Chen, C. W. Inverted colloidal crystal scaffolds with induced pluripotent stem cells for nerve tissue engineering. *Colloids Surfaces B Biointerfaces* **102,** 789–794 (2013).

47. Trombetta, R., Inzana, J. A., Schwarz, E. M., Kates, S. L. & Awad, H. A. 3D Printing of Calcium Phosphate Ceramics for Bone Tissue Engineering and Drug Delivery. *Ann. Biomed. Eng.* **45,** 23–44 (2017).

2. Aims

2. Aims

The aim of this thesis was to develop a colloidal platform able to encapsulate different types of flavonoids as quercetin and naringin and serve as a vehicle for bioinstructive cell guiding. The platform developed must be capable of sustain drug release to met applications on the fields of anti-inflammation and on fields as potentiate or promote their osteogenic differentiation. The specific aims of this master thesis were the following:

- Synthesis and characterization of dual opposite electrostatic nanoparticles;
- Synthesis and characterization of the methacrylated polymers for the nanoparticles;
- Synthesis and characterization of dual opposite electrostatic nanoparticles functionalize with methacrylate groups
- Quercetin and Naringin encapsulation and characterization of *in vitro* drug release profile;
- Evaluation of the mechanical properties of Quercetin and Naringin loaded colloidal gels;
- Evaluation of the cytotoxic profile for the colloidal gels;
- Evaluation of the antiinflammatory potential of the quercetin loaded colloidal gel;
- Evaluation of the osteogenic potential of the naringin loaded colloidal gel.

3.Results and discussion

3.1. Multicomponent Self-assembled Colloidal Gel for Focal Drug delivery

Subchapter 4.1.

This subchapter is based on the article entitled

"*Multicomponent Self-assembled Colloidal Gel for Focal Drug delivery"*

Multicomponent Self-assembled Colloidal Gel for Focal Drug delivery

Bruno Freitas, Vítor M. Gaspar[#], Pedro Lavrador and João F. Mano[#]

Department of Chemistry, CICECO – Aveiro Institute of Materials, University of Aveiro, Campus Universitário de Santiago, 3810-193, Aveiro, Portugal.

[#]Corresponding authors:
Professor Dr. João F. Mano
Department of Chemistry, CICECO – Aveiro Institute of Materials
University of Aveiro, Campus Universitário de Santiago
3810-193, Aveiro, Portugal
E-mail: jmano@ua.pt
Telephone: +351 234370733
Dr. Vítor Gaspar
Department of Chemistry, CICECO – Aveiro Institute of Materials
University of Aveiro, Campus Universitário de Santiago
3810-193, Aveiro, Portugal
E-mail: vm.gaspar@ua.pt
Telephone: +351 234370733

Abstract

Colloidal gels consisting of oppositely charged nanoparticles are being increasingly explored as controlled release depots for focal delivery in numerous tissue engineering and biomedical applications due to their dynamic physicochemical properties. In this work, we report the innovative development of a fully biodegradable colloidal gel *via* directed self-assembly of protein-rich nanogel and polymeric nanocarriers. For this purpose, a nanoprecipitation-based technique was optimized to enable the production of stable and highly monodisperse anionic Zein-Hyaluronan (Zein-HA) and cationic PLGA-Polyethylenimine (PLGA-PEI) nanocarriers, that constituted the oppositely charged building blocks. Colloidal gels self-assembly was promoted under mild physiological conditions and was confirmed by the formation of dense particle-particle networks as demonstrated by SEM and fluorescence imaging. Self-assembled colloidal gels also demonstrated moldability and fit-to-shape properties, indicating their potential to be used as bioactive tissue fillers. Gels application as focal drug delivery depots was confirmed by their significant Quercetin flavonoid encapsulation efficiency and long-term controlled release, up to 22 days. Furthermore, upon contact with LPS-activated macrophages, flavonoid-loaded colloidal gels reduced the production of nitric oxide over that of free drug, indicating the successful development of biocompatible colloidal gels for long-term focal delivery in the context of inflammation. Overall, Zein-HA/PLGA-PEI self-assembled colloidal gels moldability, and multi-particle nature, renders then promising platforms for applications spanning from focal bioactive modulators to multi-stage co-delivery systems.

Introduction

In the past years, colloidal gels have been emerging as attractive systems in tissue engineering fields due to their facile production, customizable composition and unique physicochemical properties.[1] In essence, colloidal gels comprise a continuous network of particles assembled through multiple and reversible electrostatic charge interactions.[1] These non-covalent forces, combined with its structure formed by individual nanoparticulate building blocks is responsible for their shear-thinning and self-healing characteristics. [2] These features of colloidal gels translate into injectable, moldable and fit-to-shape properties that are appealing for tissue engineering applications.[3]

Unsurprisingly, researchers have been actively pursuing novel strategies to advance colloidal gels design to develop innovative strategies. Colloidal gels structure can include polymeric, protein-based or inorganic nanoparticles that act as versatile building blocks with tailored physicochemical properties such as size, charge and surface chemistry. Also, in contrast to hydrogel networks, nanoparticles constitute superior drug depots due to their ability to load hydrophilic/hydrophobic therapeutics and to modulate their release profile. Furthermore, the coordinated assembly of different nanoparticles in the form of a colloidal gel can be used to establish programmed release rates and drug dosages that can be beneficial in complex scenarios that involve multicellular multistage processes such as wound healing, bone regeneration or inflammation. Particularly, inflammatory reactions can remain active from days, weeks, or even months, and therefore could benefit greatly from such sustained delivery depots.[4]

In the last decades, the use of anti-inflammatory molecules to modulate the inflammatory cascade as received a tremendous focus. Particularly, in recent years, flavonoids have shown remarkable potential due to their unique biocompatibility, anti-inflammatory bioactivity and natural availability.[5] In his context, Quercetin (3,5,7-trihydroxy-2-(3,4-dihydroxyphenyl)-4Hchromen-4-one), a known bioflavonoid with anti-oxidant, anti-viral, anti-inflammatory and anticancer properties has been one of the most employed.[6] However, due to its high hydrophobicity, poor gastrointestinal absorption, light-mediated degradation, as well as vulnerability to oxidation and chemical transformation in alkaline solutions, this bioactive compound has had limited success in clinical applications.[7] However, some works were able to increase its low bioavailability upon Quercetin encapsulation, increasing its stability and hence its bioactivity.[8]

Thus, the aim of this work was to develop a biodegradable colloidal gel loaded with quercetin (Gel-Q) as a drug depot with sustained flavonoid delivery for prolonged periods

of time. The developed bioactive gel was self-assembled *via* electrostatically-mediated nanoparticle aggregation under mild physiological conditions. The oppositely charged nanocarriers were comprised by FDA-approved cationic PLGA-PEI nanoparticles and corn protein-based Zein-HA nanogels loaded with Quercetin. Following colloidal gel production, its physicochemical properties in terms of water content, swelling and mass loss were evaluated. Moreover, the release profile of Quercetin-loaded colloidal gels was investigated throughout an extended time period. Afterwards, the biological performance of the bioactive gels was evaluated in *in vitro* cellular assays in terms of its cytotoxicity. Colloidal gels anti-inflammatory potential LPS-stimulated macrophages indicated their potential to promote NO_2 reduction.

2. Materials and methods

2.1. Materials

22G Stainless steel, acetone PA, Polyvinyl Alcohol (PVA), Mw 30,000-70,000, Poly(D,L-lactide-co-glycolide) (PLGA), lactide:glycolide (50:50), Mw 30,000-60,000, Poly(ethyleneimine) (PEI), branched, average Mw ~25,000 were all purchased from Laborspirit (Lisbon, Portugal). Alamar Blue, Fetal Bovine Serum (FBS), Phosphate buffered saline (PBS), Vybrant™ DiD Cell-Labeling Solution (DiD), Vybrant™ DiO Cell-Labeling Solution (DiO), Glutamax were all purchased from Thermo Fisher Scientific (Oeiras, Portugal). Antibiotic antimycotic, Dulbecco's Modified Eagle Medium (DMEM) were all purchased from Supply Center (Lisbon, Portugal). D-(+)-Trehalose Dihydrate (Trehalose) (98%), Quercetin Hydrate (96.0%), lot. XNS6N-TM, and Zein, from Corn, lot. N5JXDSK were all purchase from TCI Chemicals (Tokyo, Japan). Ethanol (99.99%) was purchased from Enzymatic, S.A. Hyaluronic acid sodium salt - Low Mw 80,000 - 100,000 (HA), batch FH634271802 was purchased from Carbosynth Limited. LPS from E. coli EH100 (Ra) TLR pure Sterile Solution (LPS) was purchased from Taper. RAW 264.7 cell line was purchased from American Type Culture Collection ® TIB-71TM

2.2. Methods

2.2.1. PLGA nanoparticles synthesis

PLGA-PEI conjugate nanoparticles (PLGA-PEI NPs) synthesis was performed by using a nanoprecipitation technique. First, 200 mg of PLGA was dissolved in 20 mL acetone. Then, the solution was transferred into a syringe and added dropwise to an aqueous phase in a 250 mL round-bottom flask under mild magnetic stirring (600 rpm). The controlled dropwise addition was performed *via* a syringe pump operating at a dropwise flux of 200 µL/min through a teflon tubbing fitted with a 22G needle for injection. The aqueous phase was comprised of 100 mL ultrapure water containing both PEI and PVA at a concentration of 0.5 % (w/v). After injection, the colloidal suspension was left stirring for 2h to form nanoparticles. Then, the solution was transferred to a rotary evaporator for 30 min, over a 40 ºC water bath and with a gradual pressure decrease to 50 mBar to minimize foam formation during this process due to the surfactant PVA. After thorough acetone evaporation, the colloidal solution was centrifuged at 18 000 g, washed with double deionized water for three times.

2.2.2. Zein nanoparticles synthesis

Zein hyaluronic acid crosslinked nanoparticles (Zein-HA NPs) synthesis was performed according to a modified nanoprecipitation technique described in the literature but with some modifications.[9] First, 200 mg of Zein was dissolved in 20 mL of ethanol (80% (v/v)). Then, the solution was transferred into a syringe and added dropwise to an aqueous phase in a 250 mL round-bottom flask under mild magnetic stirring (600 rpm). The controlled dropwise addition was performed via a syringe pump (PHD Ultra, Harvard Apparatus) operating at a dropwise flux of 200 µL/min through a teflon tubing fitted with a 22G needle for injection. The aqueous phase was comprised of 100 mL of ultrapure water containing 100 mg of HA. After injection, the colloidal suspension was left stirring for 2 h, at RT to promote nanogels formation. Then, the solution was transferred to a rotary evaporator for 30 min, over a 40 ºC water bath and with a pre-defined pressure decrease to 80 mBar. After thorough acetone evaporation, the colloidal solution was centrifuged at 18 000 g, washed with deionized water for three times. It is worth noting that the pH must be maintained at pH equal 8 throughout this process in order to reduce irreversible nanogels aggregation.

2.2.3. Nanocarriers physicochemical characterization

2.2.3.1. Dynamic light scattering

The hydrodynamic particle diameter, size distribution (PDI) and ζ-potential of different nanoparticle formulations (2 mg/mL) were characterized by dynamic light scattering (DLS) with a Zetasizer Nano ZS equipment (Malvern Instruments Ltd., Malvern, UK). All measurements were carried out in triplicate at 25 ºC, and with a 173º backscatter angle.

2.2.3.2. Scanning transmission electron microscopy

Nanoparticles size and morphology were also evaluated by Scanning Transmission Electron Microscopy (STEM). Briefly, 15 µL of NPs solution, at 2 mg/mL, were added to a Formvar film, carbon coated copper grid and then placed in the oven at 40 ºC a to dry. Image acquisition was performed in a SU-70 STEM microscope (Hitachi) operated at different accelerating voltages (e.g., 10 kV and 20 kV), and at various magnifications.

2.2.5 Colloidal Gels self-assembly

Binary colloidal gels were formed by electrostatically-driven self-assembly upon thorough mixing of anionic Zein-HA (20 mg/mL, alkaline water pH~8-9) nanoparticles with cationic PLGA-PEI (20 mg/mL, alkaline water pH~8-9) nanoparticle colloidal suspensions. The resulting Zein-HA/PLGA-PEI composites were then centrifuged at 18000g, for 15 min, at RT, to promote the formation of more compact colloidal gel.

2.2.4. Drug loading efficiency

Quercetin loaded Zein-HA nanocarriers were formulated according to the previously described nanoprecipitation/solvent evaporation methodology. For drug loaded nanoparticles manufacture 20 mg of Quercetin were dissolved in 2% Zein solution (80% ethanol) and the nanoparticles. Drug encapsulation efficiency was then determined by ultraviolet-visible (UV-Vis) spectroscopy by analysing the characteristic Quercetin flavanone peak (λ= 254 nm). This peak is followed by another region of smaller intensity to higher wavelengths (300 – 400 nm), Briefly, after Zein-HA nanoparticles centrifugation at 18000g, the supernatant was collected. For UV-vis analysis, 100 µL of particles supernatant were transferred to a quartz microplate (Helma 96-well quartz plate) and absorbance measurements were performed in a multi-purpose microplate reader (Synergy HTX). A standard calibration curve of Quercetin in ultra-pure water was used to determine the drug encapsulation efficacy (Supplementary Information, Figure S1) through the following equation:

Encapsulation efficiency was calculated using the above equation:

$$EE\% = \left(1 - \frac{\text{Amount of quercetin by indirect detection}}{\text{Theoretical amount of Quercetin added}}\right) \text{x } 100$$

2.2.5. *In vitro* drug release profile

The *in vitro* Quercetin release profile from Zein-HA/PLGA-PEI colloidal gels was performed in PBS (pH=7.4) with 0.5 % (w/v) Tween 20, at 37 ºC. Briefly, a colloidal gel was transferred to 3.5 mm PDMS mold and transferred to 50 mL Falcon and submerged into 6 mL of PBS/Tween 20 at 37 ºC in a water bath stirring at a constant rate (100 rpm). At defined time intervals, 1 mL samples were withdrawn from the solution and replaced with the same volume of fresh PBS. Samples were then centrifuged at 18000g for 15 min and analysed. A standard calibration curve in which Quercetin was left oxidizing for 2

days was used so as to account for drug oxidation in solution (Supplementary Information, Figure S2). Detection of the flavanone peak of Quercetin was obtained at (λ= 292 nm).

2.2.6. Colloidal gel characterization

2.2.6.1. Water content

For water content determination, colloidal gels were initially weighed and then frozen at -80 ºC. Fully frozen colloidal gels were then freeze dried at -86 ºC, for 1 day (LyoQuest, Telstar). The water content (WC) was calculated using the following:

$$\text{WC (\%)} = \left(\frac{Mass\ of\ eppendorf\ with\ hydrated\ gel - Mass\ of\ eppendorf}{Mass\ of\ eppendorf\ with\ freeze-dry\ gel - Mass\ of\ eppendorf}\right) \text{x } 100$$

2.2.6.2. Colloidal Gels Swelling

For swelling behaviour determination colloidal gels with defined shape were initially formed in 6 mm round PDMS mold. The resulting colloidal gel discs were then freeze-dried at -86 ºC for 1 day and weighed. For swelling experiments colloidal gel discs were placed in a 24 well plate filled with 1 mL of PBS (pH=7.4) and left at room temperature. The gels were afterwards weighed at 1, 4 and 6 h. The swelling was then calculated by using the following equation:

$$\text{SW (\%)} = \left(\frac{\text{Mass of hydrated colloidal gel}}{Mass\ of\ freeze\ dry\ colloidal\ gel}\right) \text{x } 100$$

2.2.6.3. Mass loss

Colloidal gels mass loss (ML) was determined by forming a disc shaped colloidal gel in a 6 mm round PDMS mold. The colloidal gel was then freeze-dried and weighed as before mentioned. For time course mass loss experiments colloidal composites were then placed in 1 mL of PBS (pH=7.4) and incubated in a water bath at 37 ºC. Gels mass was determined at different time points (1, 3, 5, 7 and 9 days). Mass loss was then calculated by using the following equation:

$$\text{ML\%} = \left(\frac{\text{Mass of colloidal gel at the day}}{Mass\ o\text{f hydrated colloidal gel}}\right) \text{x } 100$$

2.2.7. *In vitro* cell culture of macrophages

Raw 264.7 murine macrophages were manipulated within a Class II biological safety cabinet and maintained as per established guidelines in a humidified 5 % CO_2 atmosphere incubator at 37 ºC.[10] The cells were routinely cultured in DMEM supplemented with 10 % FBS, 1 % Glutamax and 1 % de antibiotic (Streptomycin, penicillin e gentamicin). Upon achieving 80 % to 100 % confluence, cells were scraped from the bottom of T-75 cm^2 and sub-cultured at a density of $2x10^4$ cells/cm^2.

2.2.7.1. Cytotoxicity Assays

AlamarBlue® Cell Viability assay was used for evaluation of colloidal gels and Quercetin free drug cytotoxicity. This assay is based on the metabolic reduction of the blue non-fluorescent resazurin dye to the pink-colored highly fluorescent resorufin by the mitochondrial oxidoredutase enzyme within the intracellular reducing environment of metabolically active cells.[11] For evaluation of colloidal gels and Quercetin possible cell toxicity in Raw 264.7 the cells were initially seeded overnight in a 48-well plate at a density of 10 x 10^3 cells/well, (n=6). Each plate well contained 300 µL of complete cell culture medium. In the following day colloidal gels of 3.5 mm diameter formed by blank Zein-HA/PLGA-PEI NPs or containing Quercetin loaded Zein-HA NPs were introduced in the wells. Quercetin was previously prepared as a stock solution in DMSO and was added to culture medium to a final concentration of 60 µM. During the assays, all cells were incubated for 24 and 48h After each timepoint, the DMEM medium was exchanged to DMEM containing AlamarBlue® according to manufacturer's instructions. Following an overnight incubation period, the media was then transferred to a black clear bottom 96-well plate for analysis. AlamarBlue® fluorescence was detected at an excitation/emission of λex = 540 nm/ λem = 600 nm by using a multi-mode microplate reader (Synergy HTX). All conditions were normalized to non-treated control cells.

2.2.7.2. Measurement of nitric oxide (NO) production

The production of nitric oxide (NO) by RAW 267.4 cells after LPS stimulation and in contact with Gel-Q was analysed by the Griess reagent. The colorimetric method of Griess is based on the measurement of nitrite (NO^{2-}), one of the decomposition products of NO, through the formation of an azo compound, N-alpha-naphthyl-ethylenediamine.

In short, sulphanilamide reacts with NO^{2-} which is then able to react with naphthyl-ethylenediamine, as shown in Figure.1.

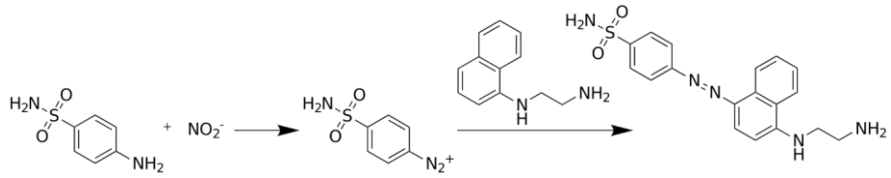

Figure 7. Schematic of Griess reaction

For NO formation quantification Raw 264.7 cells were initially seeded overnight in a48-well plates at a density of 10 x 10^3 cells/well, (n=6). In the following day all cells were incubated in DMEM containing 1 μg/mL of LPS. Subsequently, culture medium was exchanged, and Quercetin colloidal gels of 3.5 mm diameter were introduced into each well. After 2 days the DMEM medium was removed and freezed at -80 ºC for further analysis. The quantification is was performed by adding 50 μL of cell culture medium to a clear bottom 96-well plate and 50 μL of Griess reagent by a multichannel micropipette. The mixture was then incubated for 30 min, at RT. Afterwards, absorbance was read at λ = 540 nm by using a multi-mode microplate reader. All conditions were normalized to the control non-treated cells.

2.2.8. Statistical Analysis

The data obtained is expressed as the mean ± standard deviation (s.d.). Significant differences were analysed by GraphPad Prism version 7.00. One-way ANOVA was used to determine the significant differences among groups, followed by a Tukey's range test.

3. Results and Discussion

3.1. Optimization and synthesis of PLGA-PEI NPs via nanoprecipitation

PLGA is a versatile and easily tuneable biodegradable and biocompatible polyester polymer with good mechanical behaviour, which can be processed into any shape and size.[12] Moreover, PLGA nanoparticles have been widely employed as controlled drug delivery systems.[13] PEI is a biodegradable polymer with high amine density and accessible primary amine sites on the side chain making it suitable for biomedical applications where cationic charges play an important role.[14] The particles developed in this work combine the mechanical properties of PLGA particles with the highly cationic charge of PEI to create a PLGA-PEI particles with high cationic surface charge in a one pot synthesis. The cationic surface charge is highly valuable to manufacture colloidal gels.[15]

To produce large amounts of PLGA NPs required for the formulation of colloidal gels several parameters were investigated. Initially, low scale PLGA-PVA nanoparticle formulations with different PLGA concentrations were produced by nanoprecipitation. As describe previously, PLGA was dissolved in acetone and the aqueous phase remained constant at a PVA concentration of 0.5% (w/v). The F1 formulation was performed by using an air micropipette to dropwise add PLGA into the aqueous PVA solution. All other formulations were manufactured by using a peristaltic pump.

Table 1. Formulation of PLGA NPs at different conditions.

Formulation	[PLGA] (mg/mL)	Mass of polymer (mg)	Injected volume (mL)	Stabilizing solution volume (mL)	Size	PDI	Zeta
F1	2.0	4	2	8	146.4	0.059	-11,7
F2	2.0	10	5	20	130.4	0.176	-14.2
F3	2.0	40	20	100	149.4	0.14	-12.6
F4	3.5	17.5	5	20	163.4	0.065	-11.3
F5	4.0	20	5	10	213.3	0.295	-14.3
F6	20.0	100	5	20	292.9	0.091	-14.2

From F1 to F3 formulations were produced so as to evaluate the the potential for scale up. The obtained data demonstrated that an increase in volume did not change significantly NPs size, PDI or ζ-potential. Formulation F4 to F6 were formulated with

increased concentration of PLGA, this led to an increase in overall particle size and F5 formulation showed the formation of larger aggregates (also demonstrated by higher PDI). It is important to emphasize that all the conditions exhibit PDI values below the 0.2 threshold, indicating the high monodispersity of the formed nanoparticles. Moreover, PLGA-PVA nanoparticles displayed a negative zeta potential in all settings.

Following this preliminary optimization, the parameters of formulation F6 were used to evaluate nanoprecipitation into PVA-PEI aqueous mixtures so as to promote the formation of cationic PLGA nanoparticles in a one-step approach. As the results of Figure 2 demonstrate the resulting particles had a hydrodynamic diameter of ~ 208.6 nm, PDI equal to 0.063 and a surface charge, ζ-potential, of +40.4 mV.

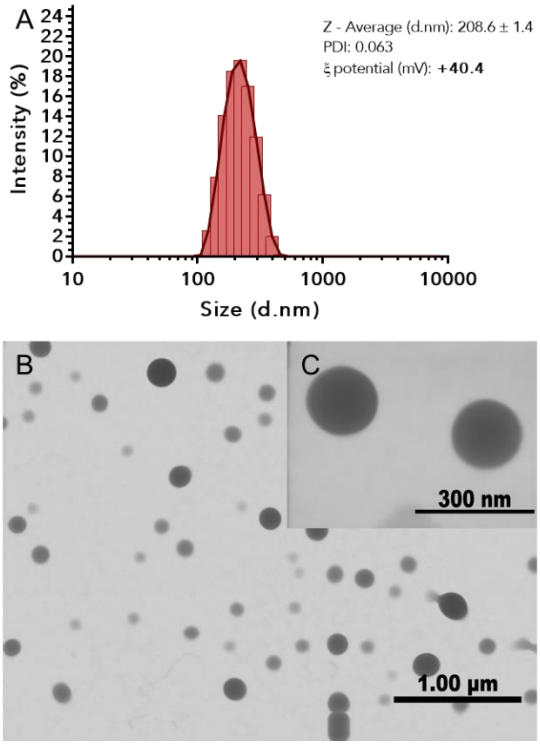

Figure 8. (A) Physicochemical characterization of PLGA-PEI NPs via DLS analysis. Each measurement was performed in triplicate and includes at least three different replicates (*n*=3). Morphological analysis through STEM at 20 kV. (B) PLGA-PEI NP (30X) and (C) PLGA-PEI NPs zoomed (200X).

The morphology of PLGA-PEI NPs was characterized by STEM and as electron microscopy micrographs demonstrate all the particles displayed well-defined spherical morphology (Figure 8 B and C).

At this point, NPs were able to be used for colloidal gels immediately after synthesis. However, aiming to increase the shelf life and storage of these nanossystems a freeze-dry

stability assay was performed. PLGA-PEI NPs (2 mg/mL) were freeze dried with Threalose as a cryoprotectant was added in values shown in table 2.

Table 2. DLS analysis of fresh and freeze dried PLGA-PEI nanoparticles in the presence of varying amounts of Threhalose cryoprotectant.

Nps	[Nps] (mg/mL)	Trehalose % (w/v)	DLS before freeze-dry			DLS after freeze-dry			DLS after freeze-dry + Wash		
			size	PdI	Zeta	size	PdI	Zeta	size	PdI	Zeta
PLGA@PEI	2	0	209.8	0.105	31.3	242.7	0.133	37.2	243.0	0.124	40.0
PLGA@PEI	2	2	215.7	0.068	28.1	220.4	0.105	39.2	216.5	0.043	45.5
PLGA@PEI	2	5	230.1	0.048	26.2	236.5	0.095	37.1	224.2	0.086	44.3

Well defined protocols for PLGA NPs freeze-dring using sucrose were already described[16], however none of them has been reported for PLGA-PEI NPs. All the obtined DLS results demonstrated an outstanding particle stability after drying. Among all the tested conditions the use of 2% (w/v) trehalose as a cryoprotectant was the most valuable since nanoparticles PDI remained the lowest (Table 2).

3.2. Synthesis of Zein-HA Protein-based NPs via nanoprecipitation

Protein-based nanocarriers are very attractable in drug delivery systems mainly due to their significant bioactivity and biocompatibility. Among the various types of proteins used for delivery systems development Zein is one of the most promising. Zein is a water-insoluble plant protein derived from maize and is divided into three types of Zein proteins: Alpha with 21–25 kDa, Beta with 17–18 kDa, and Gamma with 27 kDa. These types comprise 75–87%, 15%, and 5–10% of total natural Zein protein, respectively. The most abundant form, alpha Zein has an isoelectric point at pH = 6.8, however the surface charge of Zein can vary according to the surrounding conditions.[17] Hyaluronic acid on the other hand is a naturally occurring bioactive biopolymer capable of targetability to receptor CD44[18], is present in the extracellular matrix and it is involved in the regulation of wound healing, angiogenesis and immunomodulation.[19]

To produce Zein-HA NPs the developed nanoprecipitaion protocol was adapted from two previous reports Hae-Yong Seok *et al.*, 2018 and Mary C Regier *et al.* 2012.[18,20] Due to severe aggregation problems after centrifugation (not reported in the literature), the pH of washing solutions was modulated to increase particle repulsion and reduce aggregation This approach enabled washing and centrifugation steps. To better understand the influence of pH in Zein-HA NPs DLS analysis at various pHs was performed (Figure 3).

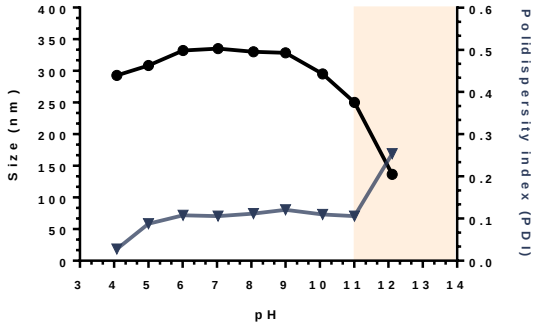

Figure 9. Zein-HA NPs colloidal suspensions was modulated from 4 to 12 using HCl and NaOH. The samples previously had gone through a DLS analysis to show the size and PDI change due to pH change.

As shown in Figure 9, Zein-HA NPs remain unusually stable up to pH=11 and at pH=12 NPs disassembled. Afterwards, 1 mL aliquots of NPs resuspended at various pHs where centrifuged 16 000g for 30 min. The full resuspension of NPs after centrifugation was only achieved at pH=8 and further, with a few large aggregates remaining at pH=7.This result determined that the optimal pH to work is pH=8. Following NPs centrifugation/washing/resuspension under optimal conditions the resulting particles showed and hydrodynamic diameter of 150.5 nm, PDI below 0.2 and a negative surface charge -44.9 mV, and displayed a spherical morphology (Figure 10 A and B).

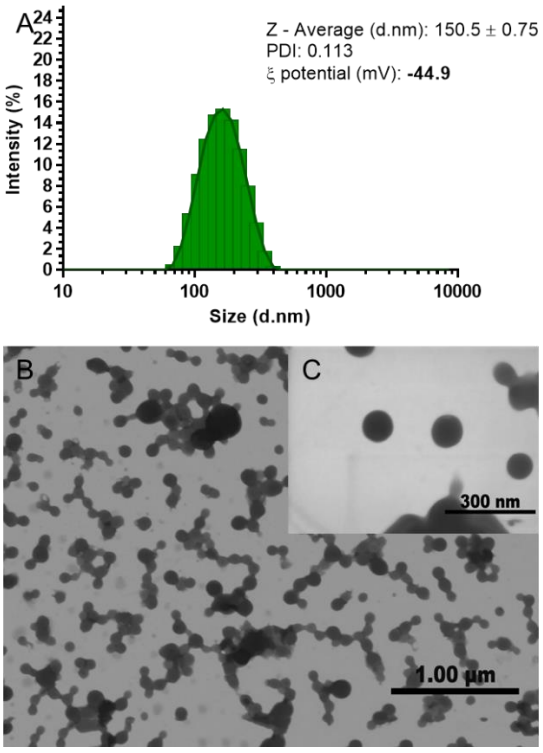

Figure 10. (A) Physicochemical characterization of Zein-HA NPs via DLS analysis. Each measurement was performed in triplicate and includes at least three different

replicates (*n*=3). Morphological analysis through STEM at 20 kV. (B) Zein-HA NP (30X) and (C) Zein-HA (200X).

Being a protein-based NP, the stability to processes such as freeze-drying is always a challenge. The aggregative nature of the Zein particles challenged us to achieve a stable formulation that could increase the shelf life of these NPs. Although the DLS results are all not so great, severe aggregation was detected in some cases (black spots) and no DLS was possible to be obtained, the 2 mg/mL of colloid concentration combined with 2% (w/v) trehalose showed the best results.

Table 3. Formulation of Zein-HA NPs were freeze-dried with different concentrations of trehalose.

Nps	[Nps] (mg/mL)	Trehalose % (w/v)	DLS before freeze dry			DLS after freeze dry		
			size	PdI	Zeta	size	PdI	Zeta
Zein@HA	1	0					1.000	
Zein@HA	2	0	147.1	0.143	-18.3		1.000	
Zein@HA	5	0					1.000	
Zein@HA	2	2	211.0	0.294	21.4	356.3	0.527	-39.1
Zein@HA	5	2				2490	0.902	-37.0
Zein@HA	2	5	3324	0.789	11.8		1.000	
Zein@HA	5	5				5703	0.753	-24.3

3.3. Quercetin Nanoparticles formulation and drug loading efficiency

As shown by the DLS results in Figure 11, particles with Quercetin have a slight increase in size and proportional decrease in surface charge when compared to their blank counterparts. This decrease can be caused by the interaction of Quercetin with hyaluronic acid.

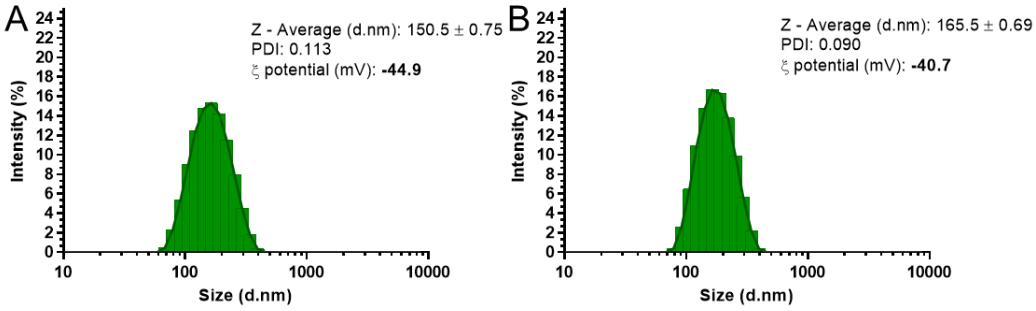

Figure 11. Physicochemical characterization of blank (A) and Quercetin-loaded (B) Zein-HA NPs via DLS analysis. Each measurement was performed in triplicate and includes at least three different replicates (n=3).

The Quercetin encapsulation efficacy in NPs was determined by UV-VIS analysis of the characteristic flavanone peak at λ= 254 nm of the aqueous solution. The obtain data

showed an encapsulation efficiency (EE) in PLGA-PEI NPs of 42 ± 4% and an EE in Zein-HA NPs of 94 ± 1%.

The encapsulation efficiency of quercetin in Zein-HA NPs was already reported in other works like that of Shuai Chen et al. 2018, with similar results that those that were found in this work. In the work of Shuai, the interaction of Quercetin with Zein and HA was evaluated The results shown an increase in Quercetin stability while in the interior of the NPS and the authors postulate that this protections could be correlated with interactions established between cathecol Quercetin group and the HA polymeric backbone.[8]

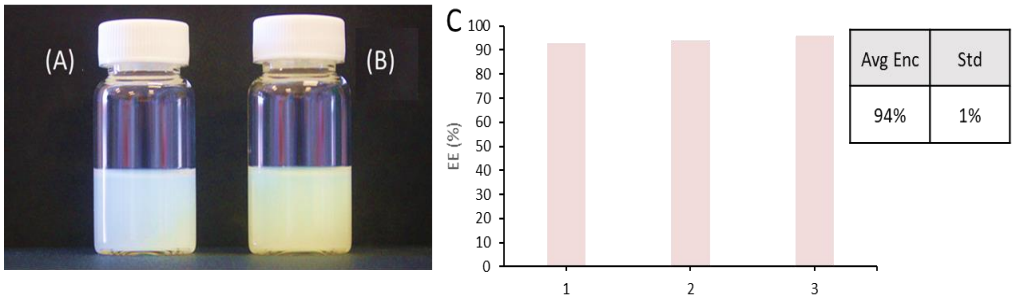

Figure 12. Zein-HA nanoparticles in suspension A) Zein-HA NPs B) Zein-HA NPs with encapsulated Quercetin. EE of Zein-HA nanoparticles encapsulation efficiency (n=3).

Moreover, encapsulation of Quercetin as already been done by other researchers using Zein NPs and different methods of NP synthesis.[8,21] All studies achieve a high encapsulation efficiency due mainly to the its high hydrophobicity and multiple coordination sites that can interact in different ways with Zein and polymer chains.[7,22,23]

3.4. Colloidal gel formation

The process of gel formation use in this work is not described in any other published reports to the best of our knowledge. The centrifugation step used herein was employed to remove most of the water and allowed the formation of a more cohesive colloidal gel than those reported.[24] At this stage the gels were inserted into round PDMS molds for subsequent tests.

As the results of figure 13 demonstrate colloidal gels were easily fitted to PDMS molds and rapidly formed cohesive networks. Interestingly the colloidal gel was easy to manipulate and remained stability in different conditions as show in Figure 14.

Figure 13. Micrographs of colloidal gel moulded to a disk shape by using a 3.5 mm PDMS mold.

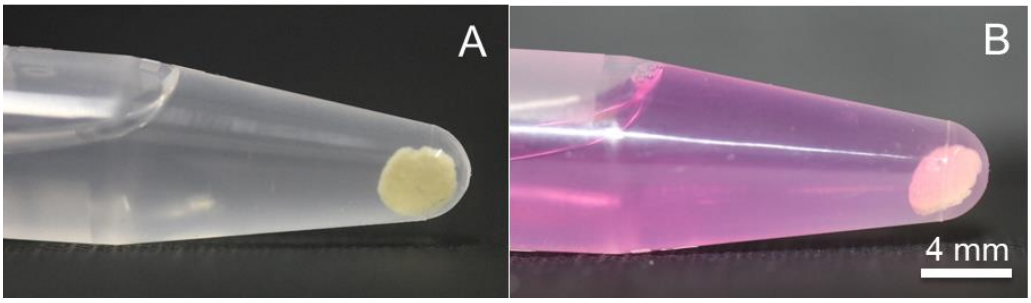

Figure 14. Colloidal gel stability when incubated in: (A) phosphate buffer and (B) culture medium.

The syringe injectability of the formed colloidal composite was confirmed as demonstrated in Figure 15. This is an important property if the focal delivery via injection is envisioned in the final application of this system as a localized long-term drug depot.

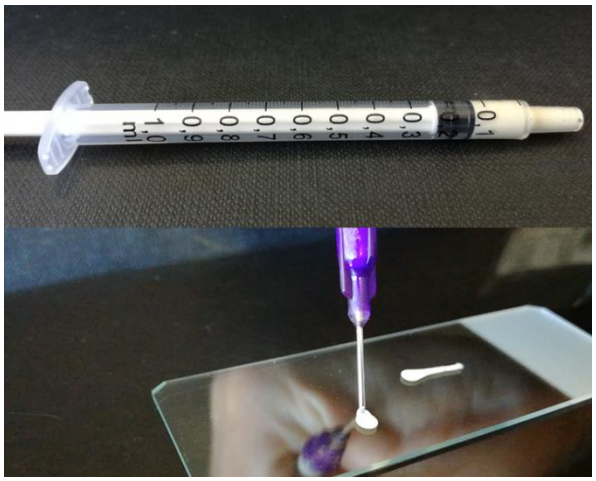

Figure 15. Colloidal gel being extruded trough a needle from an insulin syringe.

To further confirm the network dispersion of the NPs in the colloidal matrix PLGA-PEI NPs were labelled with DiD. Zein-HA NPs were labelled with DiO.

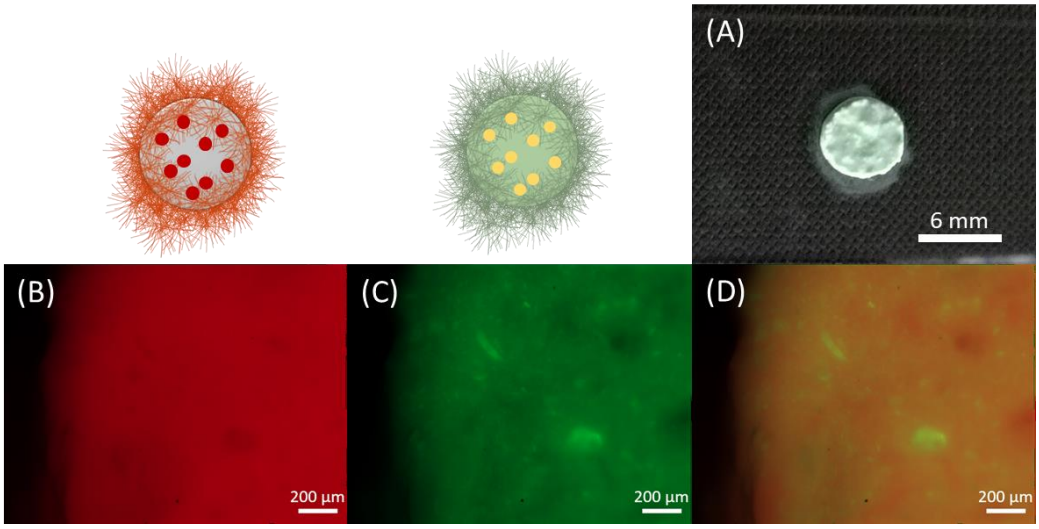

Figure 16. Fluorescence microscopy image of colloidal gels. (A) gel formed in a PDMS mold. (B) PLGA-PEI NPs labelled with DiD. (C) Microscope image of Zein-HA NPs labelled with DiO. (D) Merged channel, this shows a near complete overlap indicating an interconnecting network between the nanoparticles.

Furthermore, to evaluate the morphology of the colloidal gel network SEM images were used and as shown in Figure 17 the macro colloidal gel is formed by nanoparticle agglomerates as expected and as reported in the literature. [25]

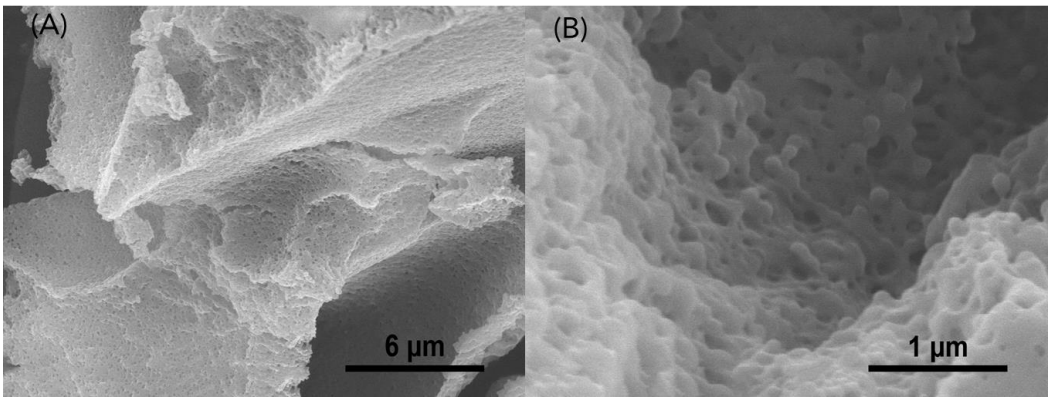

Figure 17. Morphological analysis of colloidal gel through SEM at 15 kV, A (5x) and B (30x).

3.5. Release profile of Quercetin in Gel-Q

Different factors influence drug release kinetics, the polymeric matrix and composition of the nanocarrier, its structure and biodegradation kinetics, but also the drug solubility, stability and interaction with the polymeric matrix of the nanocarrier.[26] In Quercetin's case, the flavonoid has a high hydrophobicity and low stability. In the work of Tiep Tien Nguyen et. al. 2018 the *in vitro* release was performed in PBS (pH 7.4) containing 0.5%

Tween 20 to avoid precipitation of Quercetin and retain sink conditions.[27] Herein, similar conditions were employed.

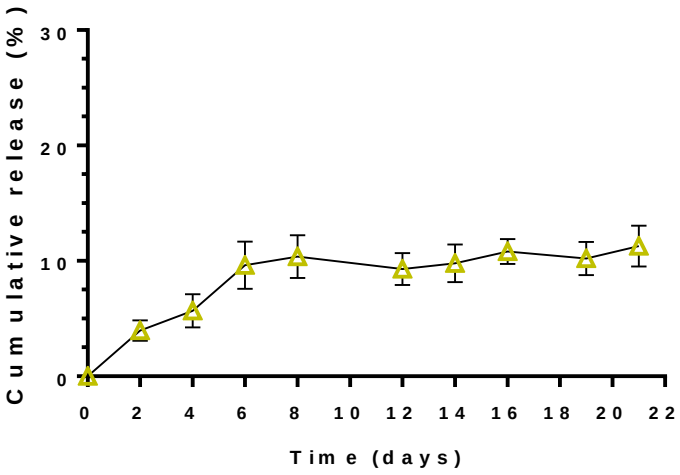

Figure 18. Cumulative release profile of Quercetin from Gel-Q in PBS at pH=7.4 containing 0.5% (w/v Tween 20). Data is presented as mean ± s.d. (*n*=3).

The obtained results clearly shown that Quercetin had a slow release up to 22 days and no significant burst release was observed. However, from a therapeutic perspective to better, this cumulative percentage is a total of approximately 140 µg of Quercetin in release medium which is a significantly higher those than that normally achieved with free nanoparticles mediated delivery.

The use of the colloidal gel in a pellet was to mimic its action *in vivo* and present a release profile from a depot perspective. The diameter and thickness of the gel influence the release rate since not only the nanocarrier but also the formed matrix serves as a diffusional barrier. Particles in center of the gel release Quercetin to the structure surrounded by other particles and were sink conditions do not exist and quercetin also as to diffuse from there.[28]

The stability of Quercetin is greatly influenced by pH, temperature, metal ions, and also other compounds such as glutathione (GSH). This short half-life is due to the hydroxyl, groups in benzene ring (A), the hydroxyketone group in pyrene ring (B) and the catechol group in benzene ring (C).[22]

For the drug detection in Uv-vis method, the degradation of quercetin had to be taken in account. Quercetin can oxidize in several forms, air oxygen present in water is usually enough or moderately alkaline solution (pH=8 to 10) can also affect Quercetin. Degradation products of quercetin usually are namely 3,4-dihydroxy-benzoic (protocatechuic) and 2,4,6-trihydroxybenzoic (phloroglucinic) acids that need to be

detected also. For that the Quercetin used for the calibration curve was left oxidizing for 2 days as this drug only needs a few hours almost fully oxidize.[29]

3.5.1. Colloidal gells Moldability and fit-to-shape potential

Moldable materials are great for multiple applications, the versatile array of shapes great interest in tissue engineering and biomedical applications.[30] The Zein-HA/PLGA-PEI gel was easily mouldable into different shapes and .

Figure 19. A colloid solution containing both NPs with food colorants of different colours to assist in seeing the moldable effect. Four different forms were made by the exertion of mechanical stress. Afterwards, they were cut in the middle and glue together with another part of other gel.

3.5.2. Colloidal gels Water content

This result demonstrates that the synthesized colloidal gel has approximately 60% (w/v) of particles to water, which is a 3-fold increase in particle concentration accounting for a more constricted network.

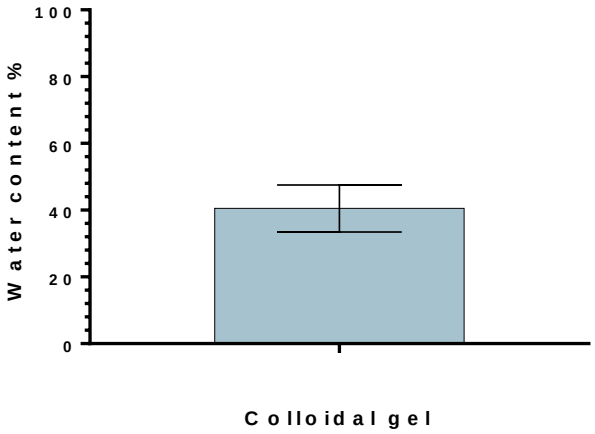

Figure 20. Water content graph represented as the ratio between the freeze-dry colloidal gel to its hydrated form after centrifugation.

3.5.3. Swelling

Swelling is the ability of a material to accumulate water in its volume. This property is important as this show how much water a system can take and see if it resists to it without structural failure.[31]

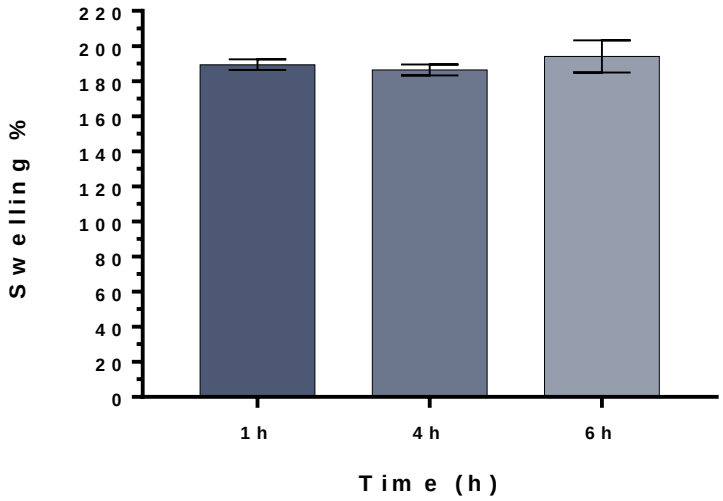

Figure 21. Swelling graph of the colloidal gel represented as the ratio between the hydrated colloidal gel at the time point to the freeze-dry colloidal gel.

After even one hour of swelling the colloidal gel retains almost its weight in water and remains for several hours with only slight increase in water uptake.

3.5.4. Mass loss

Mass loss in biomaterials is defined by the loss of material to the medium, in case of colloidal gels is the loss of particles. This property is interesting as the loss of particles can be a both a positive aspect to delivery drugs intracellularly but can also cause de breakdown of the gel at the implantation site.[32]

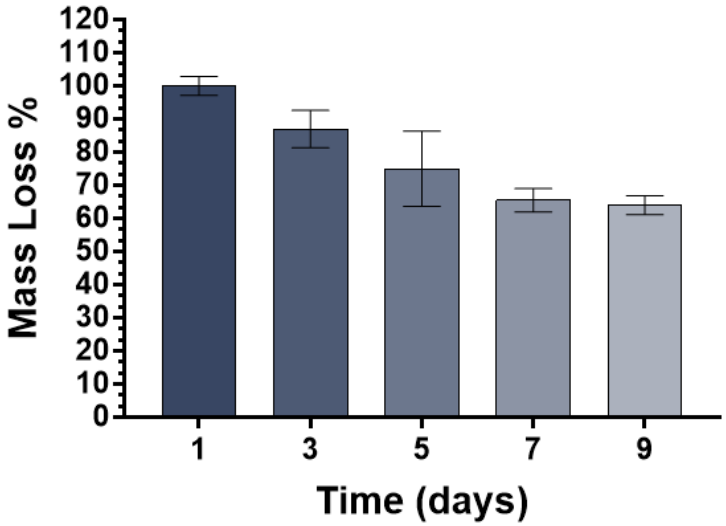

Figure 22. Mass loss graph of the colloidal gel represented as the ratio between the hydrated colloidal gel at the time point to time zero fully hydrated colloidal gel.

The mass loss of this colloidal gel is quite interesting as demonstrated in Figure 22, the gel has a significant loss of mass throughout the days. However, it seemingly remains a constant loss of particles every day,

Inflammation represents an important protective function of humans against invasion of foreign substances such as bacteria and virus or tissue injury with the intent to help the required recovery. However, when left uncheck prolonged inflammation becomes harmful and starts to damage the tissue through an excessive granulation process which diminishes subsequent tissue regeneration.[33] Cell line RAW 264.7 are a mouse macrophage cell line with response to LPS, which induced nitric oxide (NO) a crucial marker for the regulation of vascular tone, neurotransmission, acute and chronic inflammation. It´s also involved in innate immunity as a toxic agent towards infectious organisms, and can regulate the death and function of host immune cells.[34]

3.5.5. Cytotoxicity assay

An ideal colloidal gel does not exert a significant toxic effect. Blank gels, Gel-Q and Quercetin free drug effect on cell line Raw 264.7 was evaluated. Quercetin concentration was selected to 60 µM based on previous reports.[35,36,37,38]

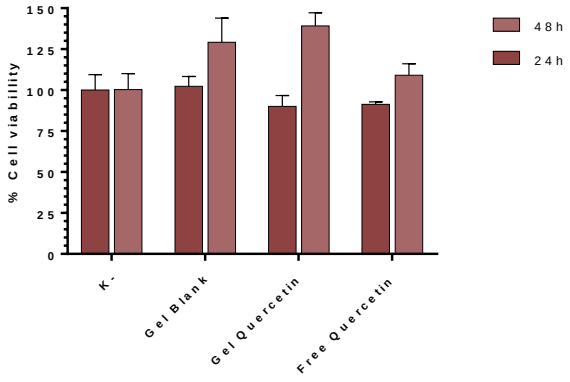

Figure 23. Characterization of the basal medium negative cytotoxicity (K-) control accounts for the 100% viability, the effect of colloidal gel and quercetin effect on Gel-Q and as free drug was evaluated.

The results demonstrate that no significant change in cell viability is obtained. These results are further complemented by optical microscopy of cells under the various conditions that display cells spreading and adhesion to the culture plate even when in culture with microgels scaffolds.

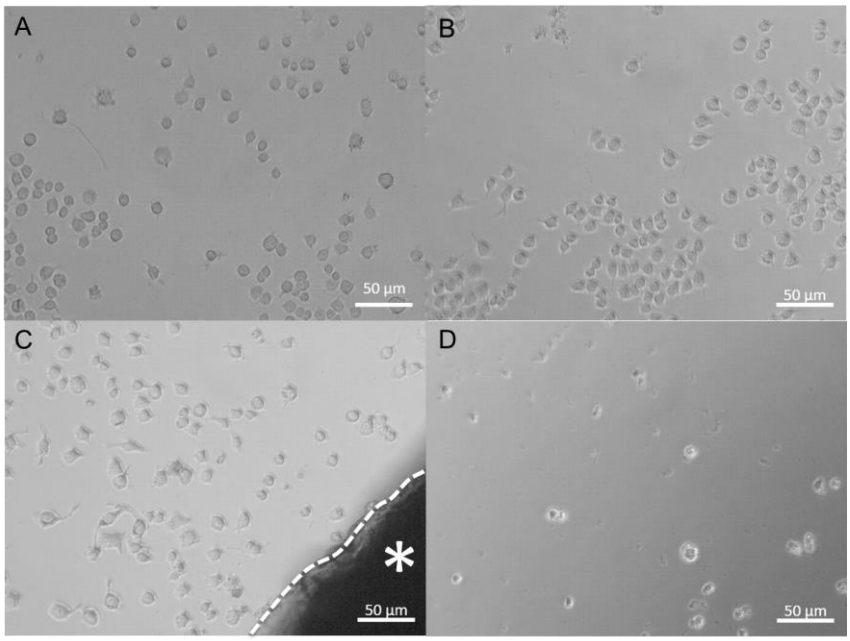

Figure 24. Raw 264.7 cells were incubated in a 48 well plate in: (A) basal medium, (B) 1µg/mL LPS-induced in DMEM culture medium, (C) 24h 1µg/mL LPS-induced in

DMEM culture medium and Gel-Q* afterward, (D) 24h 1µg/mL LPS-induced in DMEM culture medium and free drug afterward.

Inflammatory response induced with LPS resulted in an altered cell morphology as reported.[39] Cells displayed a more widespread morphology in comparison to the standard round morphology of Raw 264.7 macrophages. The main difference remaining the action of the Gel-Q with quercetin.

3.5.6. Griess assay

Griess method is a simple colorimetric assay to detect the NO production macrophages cells. The Quercetin free drug and Gel-Q formulation therapeutic effect was evaluated in LPS activated cell line Raw 264.7.

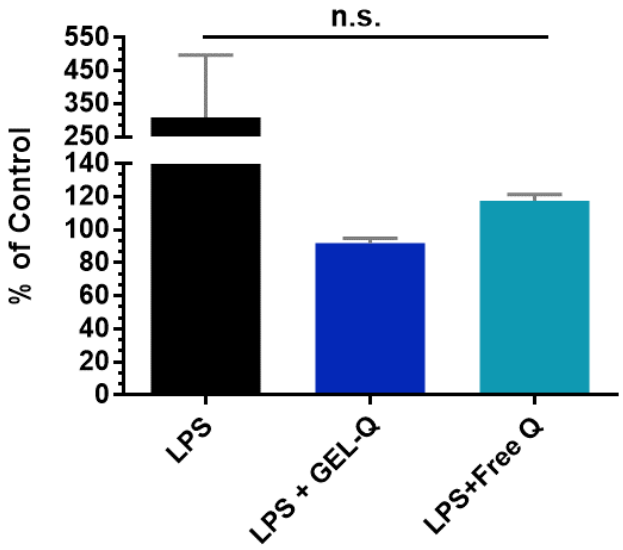

Figure 25. LPS induced NO production in Raw 264.7 macrophages. The three conditions, LPS, LPS + Gel-Q and LPS + Free Q were normalized to non-treated control cultures in basal medium. n.s. stands for non-significant, *p < 0.05. Data represented as mean ± s.d. (n=5).

The results showed some differences from Gel-Q and free drug compared to the LPS control indicating the potential of these systems to be used as drug delivery depots in the context of inflammation. These results demonstrated that the system works as an antiinflammatory platform however it requires much further studies.

4. Conclusions

In summary, this study introduced a platform for anti-inflammatory treatment using a biodegradable colloidal gel. Quercetin loaded Zein hyaluronic nanoparticles served efficiently as a nanocarrier system for drug delivery. This colloidal gel was optimized by changing the nanoparticles synthesis in both cases resulting in a colloidal gel with an incredibly precise nanoparticle dispersion. Being made of plant protein, natural polymers and biocompatible synthetic polymers makes the platform acquires multiple characteristics of each material, the plasticity from PLGA and PEI, the bioactivity and interaction of both Zein and HA.

The same colloidal gel did not pose any toxicity in Raw macrophages. The resulting colloidal gel combines the drug delivery systems of nanocarriers and extends their functionality from to a macrostructure with a cohesive network and mechanics not present in any other platform outside aa colloidal gel. The bulk structure of the gel offered a strong platform but with moldable capabilities opening exciting opportunities for advanced therapeutic applications.

Acknowledgements

The authors would like to acknowledge the support of the European Research Council grant agreement ERC-2014-ADG-669858 for project ATLAS. The authors also acknowledge the financial support by the Portuguese Foundation for Science and Technology (FCT) through a Post-doctoral grant (SFRH/BPD/119983/2016, Vítor Gaspar) and a Individual PhD grant (SFRH/BD/141834/2018, Pedro Lavrador).

5. References

1. Diba, M., Wang, H., Kodger, T. E., Parsa, S. & Leeuwenburgh, S. C. G. Highly Elastic and Self-Healing Composite Colloidal Gels. *Adv. Mater.* **29,** (2017).
2. Diba, M. *et al.* Self-Healing Biomaterials: From Molecular Concepts to Clinical Applications. *Adv. Mater. Interfaces* **5,** 1800118 (2018).
3. Mealy, J. E. *et al.* Injectable Granular Hydrogels with Multifunctional Properties for Biomedical Applications. *Adv. Mater.* **30,** 1–7 (2018).
4. Taraballi, F. *et al.* Biomimetic Tissue Engineering: Tuning the Immune and Inflammatory Response to Implantable Biomaterials. *Adv. Healthc. Mater.* **7,** 1–13 (2018).
5. Castro-Vazquez, L. *et al.* Bioactive flavonoids, antioxidant behaviour, and cytoprotective effects of dried grapefruit peels (citrus paradisi macf.). *Oxid. Med. Cell. Longev.* **2016,** (2016).
6. Tran, T. H., Guo, Y., Song, D., Bruno, R. S. & Lu, X. Quercetin-containing self-nanoemulsifying drug delivery system for improving oral bioavailability. *J. Pharm. Sci.* **103,** 840–852 (2014).
7. Li, X. *et al.* The Flavonoid Quercetin Ameliorates Liver Inflammation and Fibrosis by Regulating Hepatic Macrophages Activation and Polarization in Mice. **9,** 1–14 (2018).
8. Chen, S. *et al.* Quercetagetin-Loaded Composite Nanoparticles Based on Zein and Hyaluronic Acid: Formation, Characterization, and Physicochemical Stability. *J. Agric. Food Chem.* **66,** 7441–7450 (2018).
9. Seok, H. *et al.* CD44 targeting biocompatible and biodegradable hyaluronic acid cross-linked zein nanogels for curcumin delivery to cancer cells: In vitro and in vivo evaluation. *Journal of Controlled Release* **280,** 20–30 (2018).
10. Geraghty, R. J. *et al.* Guidelines for the use of cell lines in biomedical research. *Br. J. Cancer* **111,** 1021–1046 (2014).
11. Rampersad, S. N. Multiple applications of alamar blue as an indicator of metabolic function and cellular health in cell viability bioassays. *Sensors (Switzerland)* **12,** 12347–12360 (2012).
12. Ding, D. & Zhu, Q. Recent advances of PLGA micro/nanoparticles for the delivery of biomacromolecular therapeutics. *Mater. Sci. Eng. C* 0–1 (2018). doi:10.1016/j.msec.2017.12.036
13. Makadia, H. K. & Siegel, S. J. Poly Lactic-co-Glycolic Acid (PLGA) as biodegradable controlled drug delivery carrier. *Polymers (Basel).* **3,** 1377–1397 (2011).
14. Ma, Y. *et al.* Polyethylenimine nanofibrous adsorbent for highly effective removal of anionic dyes from aqueous solution. *Sci. China Mater.* **59,** 38–50 (2016).
15. García, M. C. & Cuggino, J. C. *Stimulus-responsive nanogels for drug delivery. Stimuli Responsive Polymeric Nanocarriers for Drug Delivery Applications, Volume 1* (Elsevier Ltd., 2018).
16. Journal, E. Freeze - drying of polycaprolactone and poly (D , L - lactic - glycolic) nanoparticles induce minor particle size changes affecting the oral pharmacokinetics of loaded drugs. **50,** 1–28 (2016).

17. Malekzad, H. *et al.* Plant protein-based hydrophobic fine and ultrafine carrier particles in drug delivery systems. *Crit. Rev. Biotechnol.* **38,** 47–67 (2018).

18. Seok, H. *et al.* CD44 targeting biocompatible and biodegradable hyaluronic acid cross-linked zein nanogels for curcumin delivery to cancer cells: In vitro and in vivo evaluation. *J. Control. Release* **280,** 20–30 (2018).

19. Bystroňová, J. *et al.* Creating a 3D microenvironment for monocyte cultivation: ECM-mimicking hydrogels based on gelatine and hyaluronic acid derivatives. *RSC Adv.* **8,** 7606–7614 (2018).

20. Regier, M. C., Taylor, J. D., Borcyk, T., Yang, Y. & Pannier, A. K. Fabrication and characterization of DNA-loaded zein nanospheres. *J. Nanobiotechnology* **10,** 1 (2012).

21. Penalva, R., González-Navarro, C. J., Gamazo, C., Esparza, I. & Irache, J. M. Zein nanoparticles for oral delivery of quercetin: Pharmacokinetic studies and preventive anti-inflammatory effects in a mouse model of endotoxemia. *Nanomedicine Nanotechnology, Biol. Med.* **13,** 103–110 (2017).

22. Pe, A., Biesaga, M. & Pyrzynska, K. Interaction of quercetin with copper ions : complexation , oxidation and reactivity towards radicals. 41–49 (2011).

23. Hajji, H. El *et al.* Interactions of quercetin with iron and copper ions : Complexation and autoxidation. **5762,** (2009).

24. Roux, R., Ladavière, C., Montembault, A. & Delair, T. Particle assemblies: Toward new tools for regenerative medicine. *Mater. Sci. Eng. C* **33,** 997–1007 (2013).

25. Wang, Q., Wang, L., Detamore, M. S. & Berkland, C. Biodegradable colloidal gels as moldable tissue engineering scaffolds. *Adv. Mater.* **20,** 236–239 (2008).

26. Fu, Y. & Kao, W. J. Drug release kinetics and transport mechanisms of non-degradable and degradable polymeric delivery systems. *Expert Opin. Drug Deliv.* **7,** 429–444 (2010).

27. Nguyen, T. T. & Jeong, J. H. Development of a single-jet electrospray method for producing quercetin-loaded poly (lactic-co-glycolic acid) microspheres with prolonged-release patterns. *J. Drug Deliv. Sci. Technol.* **47,** 268–274 (2018).

28. Siepmann, J. & Peppas, N. A. Modeling of drug release from delivery systems based on hydroxypropyl methylcellulose (HPMC). *Adv. Drug Deliv. Rev.* **64,** 163–174 (2012).

29. Zenkevich, I. G. *et al.* Identification of the products of oxidation of quercetin by air oxygen at ambient temperature. *Molecules* **12,** 654–672 (2007).

30. Oliveira, M. B., Bastos, H. X. S. & Mano, J. F. Sequentially Moldable and Bondable Four-Dimensional Hydrogels Compatible with Cell Encapsulation. *Biomacromolecules* **19,** 2742–2749 (2018).

31. Khan, F. & Tanaka, M. Designing smart biomaterials for tissue engineering. *Int. J. Mol. Sci.* **19,** 1–14 (2018).

32. Yang, R. & Liang, H. Dynamic electro-regulation of the stiffness gradient hydrogels. *RSC Adv.* **8,** 6675–6679 (2018).

33. Browne, S. & Pandit, A. Biomaterial-Mediated Modification of the Local Inflammatory Environment. *Front. Bioeng. Biotechnol.* **3,** (2015).

34. Tripathi, P., Tripathi, P., Kashyap, L. & Singh, V. The role of nitric oxide in

inflammatory reactions. *FEMS Immunol. Med. Microbiol.* **51,** 443–452 (2007).

35. Liu, H., Kao, T., Shiau, C. & Chen, B. ScienceDirect Functional components in Scutellaria barbata D . Don with anti-inflammatory activity on RAW. *J. Food Drug Anal.* **26,** 31–40 (2017).

36. Saiki, P., Nakajima, Y., Griensven, L. J. L. D. Van & Miyazaki, K. Biochemical and Biophysical Research Communications Real-time monitoring of IL-6 and IL-10 reporter expression for anti-in fl ammation activity in live RAW 264 . 7 cells. *Biochem. Biophys. Res. Commun.* **505,** 885–890 (2018).

37. Endale, M. *et al.* Immunobiology Quercetin disrupts tyrosine-phosphorylated phosphatidylinositol 3-kinase and myeloid differentiation factor-88 association , and inhibits MAPK / AP-1 and IKK / NF- □ B-induced inflammatory mediators production in RAW 264 . 7 cells. *Immunobiology* **218,** 1452–1467 (2013).

38. Maurya, A. K. & Vinayak, M. Improved synergistic anticancer efficacy of quercetin in combination with PI-103 , rottlerin , and G0 6983 against MCF-7 and RAW 264 . 7 cells. (2018).

39. Remppis, A. *et al.* Rhizoma coptidis inhibits LPS-induced MCP-1/CCL2 production in murine macrophages via an AP-1 and NF B-dependent pathway. *Mediators Inflamm.* **2010,** (2010).

6. Annexes

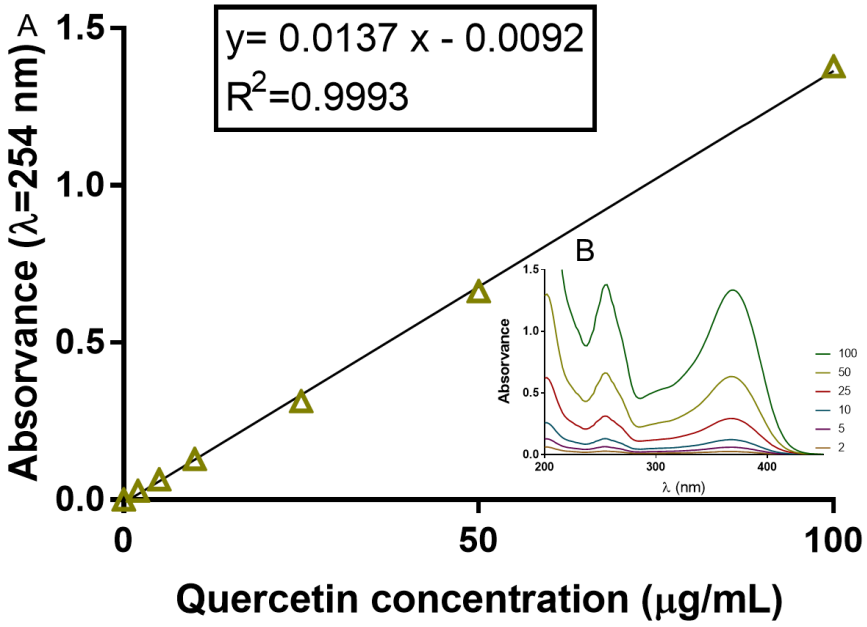

Figure 26. (A) Quercetin calibration curve in water calculated by measuring the absorbance peak at λ =254 nm, ranging from 2 – 100 μg/mL. (B) Inset represents the absorbance spectrum of Quercetin within a spectral window of 200 to 450 nm.

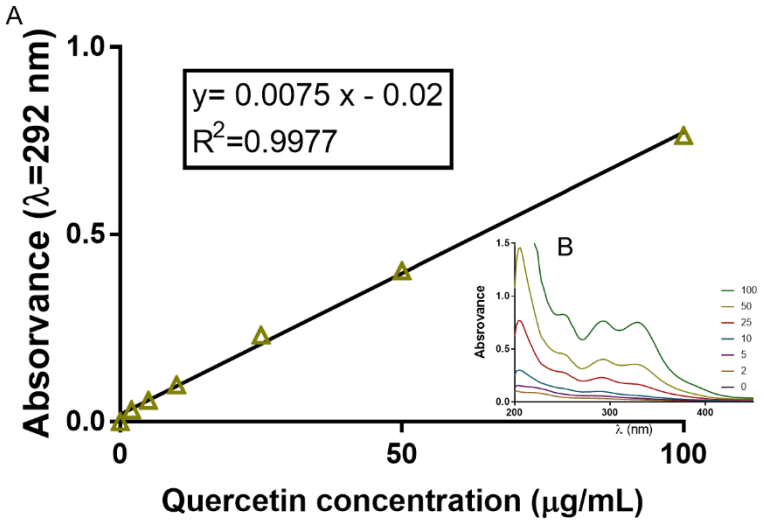

Figure 27. (A) Quercetin calibration curve in Pbs-Tween 20 calculated by measuring the absorbance peak at λ =292 nm, ranging from 2 – 100 μg/mL. (B) Inset represents the absorbance spectrum of Quercetin within a spectral window of 200 to 450 nm.

3.2. *In situ* photocrosslinkable double-network colloidal gel as injectable bioactive depots for tissue engineering

Subchapter 4.2.

This subchapter is based on the article entitled

"*In situ photocrosslinkable double-network colloidal gel as injectable bioactive depots for tissue engineering"*

In situ photocrosslinkable double-network colloidal gel as injectable bioactive depots for tissue engineering

Bruno Freitas, Vítor M. Gaspar#, Pedro Lavrador and João F. Mano#

Department of Chemistry, CICECO – Aveiro Institute of Materials, University of Aveiro, Campus Universitário de Santiago, 3810-193, Aveiro, Portugal.

#Corresponding authors:
Professor Dr. João F. Mano
Department of Chemistry, CICECO – Aveiro Institute of Materials
University of Aveiro, Campus Universitário de Santiago
3810-193, Aveiro, Portugal
E-mail: jmano@ua.pt
Telephone: +351 234370733
Dr. Vítor Gaspar
Department of Chemistry, CICECO – Aveiro Institute of Materials
University of Aveiro, Campus Universitário de Santiago
3810-193, Aveiro, Portugal
E-mail: vm.gaspar@ua.pt
Telephone: +351 234370733

Abstract

Colloidal gels are attractive platforms comprising a continuous network of assembled particles in an arrested state that can yield multifunctional materials with tunable mechanical properties and controlled delivery of bioinstructive agents. In this work, we report for the first time the development of a double-network colloidal gel system encompassing a combination of plant protein-based and polymeric nanoparticles. A robust and modified nanoprecipitation technique enabled the production of stable and monodisperse Zein and PLGA nanoparticles coated with outer shells of hyaluronic acid and polyethylenimine, respectively Zein-HAm and PLGA-PEIm, containing different degrees of pendant methacrylated groups (35% and 19% correspondingly). The external coating allowed dense photocrosslinking at the nanoscale interconnecting the entire colloidal gel network and yielding robust and stable double-network colloidal gels. Scanning electron microscopy confirmed the nanoparticle-laden nature of the gels. Furthermore, the double-network colloidal gels contained equal amounts of water-to-nanoparticles and were highly stable in physiological conditions, showing no appreciable mass loss over the course of two weeks, especially in comparison to the more fragile single network colloidal gels. Additionally, bioinstructive Naringin was encapsulated within this nanoparticulate gel, where it was shown that flavonoid-containing gels were biocompatible and enhanced osteogenesis over free drug. This work represents the first successful development of double-network colloidal gels, a versatile platform for tissue engineering trends with improved robustness and flexible biofunctionality derived from the plethora of bioactive molecules that can be incorporated in these systems via nanoparticle entrapment.

1. Introduction

Colloidal gels are defined as a three-dimensional network of assembled particles in an arrested state. Colloids and proteins acquire distinct charges when dispersed in aqueous solutions, increasing electrostatic interactions among themselves and directing self-assembly if significant proportions of opposite charges are present [1]. Dynamical arrest is associated with structural transitions in the gel network derived from directed percolation phenomena that occur because polymer-free volume is maximized when colloids approach one another [2]. In the gel region, the colloidal system is then trapped in a local energy minimum, becoming arrested and unable to undergo any additional structural transition unless external events occur [3]. This process can resemble the biological mechanisms found in protein folding and plaque formation [2]. Ultimately, colloidal gel formation is governed by supramolecular interactions and can thus be quantitatively driven by the number of bonded neighbors [3].

In classic delivery systems, nanoparticle aggregation is a serious problem affecting the performance of several formulations, whereas in the perspective of colloidal gels this behavior is encouraged and extensively pursued [4–6]. Indeed, in the latter, researchers also carefully balance nanoparticles surface charge, size, polydispersity as well as optimize surfactant quantities, but this strategy is done towards the goal of achieving self-assembled colloidal gel systems [7–9]. In some cases, the resulting percolating self-sustained microstructure can resemble macroscopic structures found in nature, in particular those of aggregate fruits such as raspberries [10].

The unique mechanical properties attributed to colloidal gels stem from the percolating network and the hydrodynamic interplay between the various colloids and solvent [11]. Due to its dynamic self-assembly nature via nanoparticle aggregation, these gels can readily undergo shear-thinning under pressure or self-heal by the nanosized monomers movement within the network [12,13]. Therefore, colloidal gels possess attractive features for tissue engineering strategies with their intrinsic injectable and moldable behaviors [12,14]. Also, critical aspects such as biocompatibility and biodegradability are necessary when designing implantable platforms, and these properties can be guaranteed in colloidal gels owing to its customizable fabrication process that can encompass several polysaccharide-based, protein-based or FDA-approved polymeric building blocks [15–18]. Moreover, inherent to its

nanoparticle-laden nature, these colloidal gels can include a plethora of bioinstructive agents and achieve sustained release patterns, thus providing localized bioactive depots that are also attractive for advanced regenerative medicine applications [19–21].

However, current iterations of colloidal gels are characterized by poor mechanical properties, due to the overwhelming majority of studies focusing mainly on electrostatic interactions to drive the assembly of colloidal gels [12]. Indeed, such constructs show both injectable and moldable potential, but suffer from insufficient stiffness and stability properties that hinder realistic applications for injectable drug delivery platforms or moldable tissue engineering constructs [13]. In the latter, the ability to remain localized at the injection site and withstand biological flow as well as mechanical loading is critical for successful translation [22]. More recently, a colloidal gel with improved mechanical robustness and self-healing capacity was developed by combining different-sized nanoparticles of silica (80 nm) and gelatin (400 nm) [13]. Still surprisingly, in the field of colloidal gels, the potential for introducing reversible dynamic covalent bonds or stimuli-responsive covalent crosslinking is still vastly underexplored. Designing such smart platforms can greatly improve drug release profiles, as well as endow controllable mechanical and self-healing properties to manufacture the next-generation of advanced colloidal gels.

In this work, a modified nanoprecipitation method enabled a one-step preparation of nanosized colloids with a simultaneous outer coating containing homogeneous polymeric layers. Moreover, its high-throughput potential, scalable features as well as the capacity for affording highly monodisperse colloids, represent an attractive tool for fabricating novel colloidal gels with user-defined compositions, physicochemical performances and multivalent bioactivities. Pre-functionalization with pendant methacrylic groups in outer polymeric brushes covering the nanoparticles offers an on-demand, smart crosslinking of the colloidal gel network previously formed via electrostatically-attracted nanossystems. Here, the first network acts as a flexible template that enables shaping and molding to fill complex defect sites or inclusion within sophisticated tissue engineering platforms. Then, the hardening of the colloidal gel is achieved by photocrosslinking of the methacrylated groups, gluing the system by installing a double-network that intertwines the entire structure, thus yielding robust and interconnected colloidal gels *in situ*. Furthermore, the inherent capacity of nanoparticles to hold and release multiple bioactive molecules expand the applications of this nanoparticle-laden gel to fulfil several healthcare purposes.

2. Materials and methods

2.3. Materials

Hydroxy-4'-(2-hydroxyethoxy)-2-methylpropiophenone (Irgacure), 1-(3-Dimethylaminopropyl)-3-ethylcarbodiimide (EDC), 22G Stainless steel, acetone PA, Polyvinyl Alcohol (PVA), Mw 30,000-70,000, 4-Nitrophenol 10 mM (4NPh), 4-Nitrophenyl phosphate disodium salt hexahydrate (4NPhP), Triton X-100 BioXtra, Naringin (≥95%), lot. BCBQ1754V, Poly(D,L-lactide-co-glycolide) (PLGA), lactide:glycolide (50:50), Mw 30,000-60,000, Poly(ethyleneimine) (PEI), branched, average Mw ~25,000 were all purchased from Laborspirit (Lisbon, Portugal). Alamar Blue, Fetal Bovine Serum (FBS), Phosphate buffered saline (PBS), Vybrant™ DiD Cell-Labeling Solution (DiD), Vybrant™ DiO Cell-Labeling Solution (DiO) and Dexamethasone (Dex, 96% purity, ACROS Organics™) were all purchased from Thermo Fisher Scientific (Oeiras, Portugal). Antibiotic antimycotic, α-MEM powder (-nucleosides, +L-glutamine) (αMEM) were all purchased from Supply Center (Lisbon, Portugal). D-(+)-Trehalose Dihydrate (Trehalose) (98%), N-Hydroxysuccinimide (NHS), Methacrylic acid (MA), Glycidyl methacrylate (GM) and Zein, from Corn, lot. N5JXDSK were all purchase from TCI Chemicals (Tokyo, Japan). Ethanol (99.99%) was purchased from Enzymatic, S.A. Hyaluronic acid sodium salt - Low Mw 80,000 - 100,000 (HA), batch FH634271802 was purchased from Carbosynth Limited. LPS from E. coli EH100 (Ra) TLR pure Sterile Solution (LPS) was purchased from Taper. L-ascorbic acid 2-phosphate magnesium salt (AA) was purchased from VWR. β-glycerophosphate disodium salt hydrate (BG) was purchased from Santa Cruz Biotechnology. Human adipose derived mesenchymal stem cells (hASCs, Homo Sapiens, ATCC® PCS-500-011™) were purchased from LGC Standards S.L.U. (Barcelona, Spain).

2.4. Methods

2.4.1. Polymer synthesis

2.4.1.1. PEI methacrylate

The modification of PEI was achieved by dissolving 2 g of PEI in 30 mL of MES buffer (pH=6). The solution was poured into a 100 mL round bottom flask protected from light. In separate, 3.300 g of EDC and 1.650 g of NHS were dissolved in 20 mL of MES buffer. To this mixture 1.2 mL of MA was added under vortex mixing (exothermic reaction) and poured immediately into a 100 mL flask containing 2 g of PEI in MES. The reaction proceeded for

24 h in under 400 RPM magnetic stirring (magnetic bar dimension, 30x5 mm). Subsequently, the resulting PEI-methacrylate (PEIm) was transferred to a regenerated cellulose dialysis membrane (MWCO ~3500 Da) and dialyzed against deionized water for 3 days. The purified polymer was then frozen at -80 ºC and freeze dried for 5 days by the end of which a cotton-like polymer was obtained.

2.4.1.2. Hyaluronic Acid methacrylate

The modification of hyaluronic acid (HA) was achieved by initially dissolving 2 g of HA in 100 mL of deionized water. The solution was then poured into a 500 mL round bottom flask protected from light, after which 100 mL DMF, 35 mL of TEA and 34 mL of GM were added. The reaction occurred for 72 h in a magnetic plate at 400 RPM (magnetic bar dimension, 30x5 mm). Subsequently, the modified polymer was transferred to regenerated cellulose dialysis membrane (MWCO ~3500 Da) and dialyzed for 5 days by using water as a dialysis solution. The resulting polymer methacrylated HA (HAm) was placed at -80ºC and freeze dried to obtain a cotton shape foam that was stored in a desiccator, at room temperature (RT) until further use.

2.4.2. PLGA-PEI methacrylate nanoparticles synthesis

PLGA-PEI methacrylate conjugate nanoparticles (PLGA-PEIm NPs) synthesis was performed by using a nanoprecipitation technique. First, 200 mg of PLGA was dissolved in 20 mL acetone. Then, the solution was transferred into a syringe and added dropwise to an aqueous phase in a 250 mL round-bottom flask under mild magnetic stirring (600 rpm). The controlled dropwise addition was performed via a syringe pump operating at a dropwise flux of 200 µL/min through a teflon tubbing fitted with a 22G needle for injection. The aqueous phase was comprised of 100 mL ultrapure water containing both PEIm and PVA at a concentration of 0.5 % (w/v). After injection, the colloidal suspension was left stirring for 2h to form nanoparticles. Then, the solution was transferred to a rotary evaporator for 30 min, over a 40 ºC water bath and with a gradual pressure decrease to 50 mBar to minimize foam formation during this process due to the surfactant PVA. After thorough acetone evaporation, the colloidal solution was centrifuged at 18 000 g, washed with double deionized water for three times.

2.4.3. Zein-Hyaluronic acid methacrylate nanoparticles synthesis

Zein hyaluronic acid methacrylate nanoparticles (Zein-HAm NPs) synthesis was performed according to a modified nanoprecipitation technique described in the literature but with some modifications. First, 200 mg of Zein was dissolved in 20 mL of ethanol (80% (v/v)). Then, the solution was transferred into a syringe and added dropwise to an aqueous phase in a 250 mL round-bottom flask under mild magnetic stirring (600 rpm). The controlled dropwise addition was performed via a syringe pump (PHD Ultra, Harvard Apparatus) operating at a dropwise flux of 200 µL/min through a teflon tubing fitted with a 22G needle for injection. The aqueous phase was comprised of 100 mL of ultrapure water containing 100 mg of HAm. After injection, the colloidal suspension was left stirring for 2 h, at RT to promote nanogels formation. Then, the solution was transferred to a rotary evaporator for 30 min, over a 40 ºC water bath and with a pre-defined pressure decrease to 80 mBar. After thorough acetone evaporation, the colloidal solution was centrifuged at 18 000 g, washed with deionized water for three times. It is worth noting that the pH must be maintained at pH equal 8 throughout this process in order to reduce irreversible nanogels aggregation.

2.4.4. Physicochemical Characterization of nanoparticles

2.4.4.1. Dynamic light scattering

The hydrodynamic particle diameter, size distribution (PDI) and ζ-potential of different nanoparticle formulations (2 mg/mL) were characterized by dynamic light scattering (DLS) with a Zetasizer Nano ZS equipment (Malvern Instruments Ltd., Malvern, UK). All measurements were carried out in triplicate at 25 ºC, and with a 173º backscatter angle.

2.4.4.2. Scanning transmission electron microscopy

Nanoparticles size and morphology were also evaluated by Scanning Transmission Electron Microscopy (STEM). Briefly, 15 µL of NPs solution, at 2 mg/mL, were added to a Formvar film, carbon coated copper grid and then placed in the oven at 40 ºC a to dry. Image acquisition was performed in a SU-70 STEM microscope at different accelerating voltages (e.g., 10 kV and 20 kV), and at various magnifications.

2.4.4.3. FTIR-ATR Spectroscopy

To further confirm the presence of conjugated polymers in the particles, NPs were centrifuge at 18000 g. The resulting pellets were then placed in the oven at 40ºC and let overnight to dry. The sample was analyzed by FTIR-ATR spectroscopy. The spectra of all samples were recorded at a 2 cm^{-1} resolution for a total of 256 scans in the spectral width of 3000 to 350 cm^{-1}. The spectra were obtained and processed in OPUS software.

2.4.4.4. Drug loading efficiency

Drug encapsulation efficiency was determined by ultraviolet-visible (UV-VIS) absorbance of the flavanone peak of Naringin (λ= 282 nm). This peak is followed by another region of smaller intensity to higher wavelengths (300 – 400 nm), Briefly, after centrifuge at 18000 g, free drug in solution is measured, Naringin-loaded nanoparticles remain in the form of pellet and are not quantified. For UV-vis analysis, 100 µL of particles supernatant were transferred to a quartz microplate (Helma 96-well quartz plate) and absorbance measurements were performed in a multi-purpose microplate reader (Synergy HTX). A standard calibration curve of naringin in ultra-pure water was used to determine the drug encapsulation efficacy (Annex, figure S3).

Encapsulation efficiency was calculated using the following equation:

$$EE\% = \left(1 - \frac{\text{Amount of Naringin by indirect detection}}{\text{Theoretical amount of Naringin added}}\right) \times 100$$

2.4.4.5. Colloidal gel formation

Binary colloidal gels were formed by electrostatically-driven self-assembly upon thorough mixing of anionic Zein-HAm (20 mg/mL, alkaline water pH~8-9) nanoparticles with cationic PLGA-PEIm (20 mg/mL, alkaline water pH~8-9) nanoparticle colloidal suspensions. The resulting Zein-HAm/PLGA-PEIm composites were then centrifuged at 18000g, for 15 min, at RT, to promote the formation of more compact colloidal gel. Secondary crosslinking was performed by including 1% (w/v) Irgacure in alkaline solution before particles centrifugation. The electrostatically agglomerated colloidal gels were then transferred to 3.5 mm PDMS round molds and irradiated with U.V. light at 3.71 W/cm^2 for 5 min (Omnicure UV lamp, S2000).

2.4.4.6. Naringin *in vitro* release profile

The *in vitro* Naringin release profile from the gel was investigated in a solution of PBS with 0.5% (w/v) Tween 20 to mimic the physiological scenario, pH 7.4 (physiological pH). Briefly, a colloidal gel made from a PDMS mold with 3.5 mm punch after freeze-drying was weighted and was transferred to 50 mL Falcon and submerged by 6 mL of PBS/Tween 20 at 37 ºC in the water bath at a constant stirring rate (100 rpm). At defined time intervals, 1 mL samples were withdrawn from the solution and replaced with the same volume of fresh PBS. Samples were quickly centrifuge at 18000g for 15 min and quickly analyze. Detection of the flavanone peak of Naringin occurred at absorbance of (λ= 282 nm). A standard calibration curve of Naringin in H_2O was used (Annex, figure S3).

6.1.1.1. Water content

For water content determination, colloidal gels were initially weighed and then frozen at -80 ºC. Fully frozen colloidal gels were then freeze dried at -86 ºC, for 1 day (LyoQuest, Telstar). The water content (WC) was calculated using the following:

$$\text{WC (\%)} = \left(\frac{Mass\ of\ eppendorf\ with\ hydrated\ gel - Mass\ of\ eppendorf}{Mass\ of\ eppendorf\ with\ freeze-dry\ gel - Mass\ of\ eppendorf}\right) \text{x } 100$$

6.1.1.2. Colloidal Gels Swelling

For swelling behaviour determination colloidal gels with defined shape were initially formed in 6 mm round PDMS mold. The resulting colloidal gel discs were then freeze-dried at -86 ºC for 1 day and weighed. For swelling experiments colloidal gel discs were placed in a 24 well plate filled with 1 mL of PBS (pH=7.4) and left at room temperature. The gels were afterwards weighed at 1, 4 and 6 h. The swelling was then calculated by using the following equation:

$$\text{SW (\%)} = \left(\frac{\text{Mass of hydrated colloidal gel}}{Mass\ of\ freeze\ dry\ colloidal\ gel}\right) \text{x } 100$$

6.1.1.3. Mass loss

Colloidal gels mass loss (ML) was determined by forming a disc shaped colloidal gel in a 6 mm round PDMS mold. The colloidal gel was then freeze-dried and weighed as before mentioned. For time course mass loss experiments colloidal composites were then placed in 1 mL of PBS (pH=7.4) and incubated in a water bath at 37 ºC. Gels mass was determined at different time points (1, 3, 5, 7 and 9 days). Mass loss was then calculated by using the following equation:

$$\text{ML\%} = \left(\frac{\text{Mass of colloidal gel at the day}}{Mass\ of\ \text{hydrated colloidal gel}}\right) \text{x } 100$$

2.4.5. Cell culture of Human adipose derived stem cells (ASCs)

All cells were manipulated within a Class II biological safety cabinet and maintained as per established guidelines in a humidified 5 % CO2 atmosphere incubator with 95 % O_2 and at 37 ºC.[23] ASCs were routinely cultured in α-MEM supplemented with 10

% (v/v) heat-inactivated FBS and 1 % of antibiotic mixture as basal medium (BM) and for osteogenic differentiation (OM), 50 μg/mL of AA, 10 mM of BG and 10 mM Dex. AA, BG and Dex are prepared previously in DMSO and stored in aliquots, upon addition to basal medium DMSO accounts for 0.1 % (v/v) across all concentrations. All assays were made in 48 well plates with 300 μL of culture medium and subcultured after reaching 80% to 100% confluence.

2.4.5.1. Cytotoxicity Assays

Assessment of cell metabolism of ASCs was performed by using the AlamarBlue® Cell Viability assay. This assay is based on the metabolic reduction of the blue non-fluorescent resazurin dye to the pink-colored highly fluorescent resorufin by the mitochondrial oxidoredutase enzyme within the intracellular reducing environment of metabolically active cells.[24] For evaluation of colloidal gels and naringin possible cell toxicity in Raw 264.7 cells were initially seeded overnight in a48-well plate at a density of 10 x 10^3 cells/well, (n=6). Each plate well contained 300 μL of supplemented DMEM. Then, cells were presented to different colloidal gels. Colloidal gels of 3.5 mm diameter blank or with naringin loaded were introduce in the well. During the assays, all cells were incubated for 24 and 48h. Naringin was previously prepared as a stock solution in DMSO and was added to culture medium in the ratio of 1:1000 to a final concentration of 60 μM. After each timepoint, the DMEM was exchanged to DMEM containing AlamarBlue according to manufacturer's instructions. Following an overnight incubation period, the media was then transferred to a black clear bottom 96-well plate for analysis. AlamarBlue fluorescence was detected at an excitation/emission of λex = 540 nm/ λem = 600 nm by using a multi-mode microplate reader. All conditions were normalized to the control group set at 100 % viability.

2.4.5.2. ALP Activity measurement assay

The ability of Naringin present in the colloidal gel to induce osteogenic differentiation of ASCs was evaluated in OM. ASCs were seeded overnight in a 48-well culture plate at a

density of 3.5 x 10^3 cells/well (*n*=5) in 300 µL of BM. After 24h of cell seeding, medium was replaced with basa medium (BM), osteogenic medium (OM), OM with Naringin in colloidal gel (Gel-Nar) and OM-Nar containing free Naringin at a concentration of 50 µg/mL, in a single dose. All cells were incubated for 7 and 14 days and the respective differentiation medium was exchanged every 3 to 4 days.

For ALP quantification cells were initially lysed by using the freeze-thaw technique to release ALP enzyme to the extracellular medium. Initially, cells were washed twice with dPBS and incubated with 300 µL of 2 % Triton X-100 solution in deionized water in an ultrasound bath for 7 min (37 Hz, sweep field, 60 % potency) before being frozen at -20 ºC. This freeze-thaw cycle was repeated one more time before determining ALP activity in the lysates by using 4NPhP ALP-mediated hydrolysis to quantify 4NPh release. For this quantification, 25 µL of each lysate sample were added to 75 µL of a freshly prepared 4NPhP solution (2 mg/mL) in 1 M diethanolamine (DEA) buffer (pH 9.8, with 0.5 mM MgCl2). The samples were incubated in the dark at 37 ºC for 1 h. Enzyme activity was then quantified by UV-VIS analysis at λ = 405 nm. A standard curve of 4NPh was used as reference (0, 15 30, 50, 75, 95 µM in DEA buffer). The ALP activity was normalized according to the total DNA content in cell lysate determined by a PicoGreen® DNA Quantification kit according to the aforementioned protocol, and ALP was expressed as nanomole of p-nitrophenol/pg dsDNA.

2.4.5.3. Statistical Analysis

The data obtained is expressed as the mean ± standard deviation (s.d.). Significant differences were analysed by GraphPad Prism version 7.00. One-way ANOVA was used to determine the significant differences among groups, followed by a Newman-Keuls multiple comparison test for pairwise comparison.

3. Results and Discussion

3.3. PEI methacrylate synthesis

Poly(ethylene imine) (PEI) is a polymer synthesized via acid-catalyzed cationic ring-opening polymerization of the ethylene imine monomer. This process leads to the formation of an hyperbranched structure containing primary, secondary, and tertiary amino units.[25] This branch rich in amines are ideal chemically active sites due to their reactivity and can be easily modified.[26] Herein, EDC/NHS was used to activate the carboxylic acid in methacrylate to obtain modified PEIm. The ^{1}H NMR spectra (Figure 26) and FTIR (Figure 27) indicate that the reaction was successful and that the polymers have a significant degree of functionalization.

In the ^{1}H NMR spectrum of methacrylated hyaluronic acid, two new peaks with a chemical shift of δ=5.4 and δ=5.8 ppm were obtained. These peaks are characteristic of methacrylate vinyl groups (Figure 1, Peak A).[27]

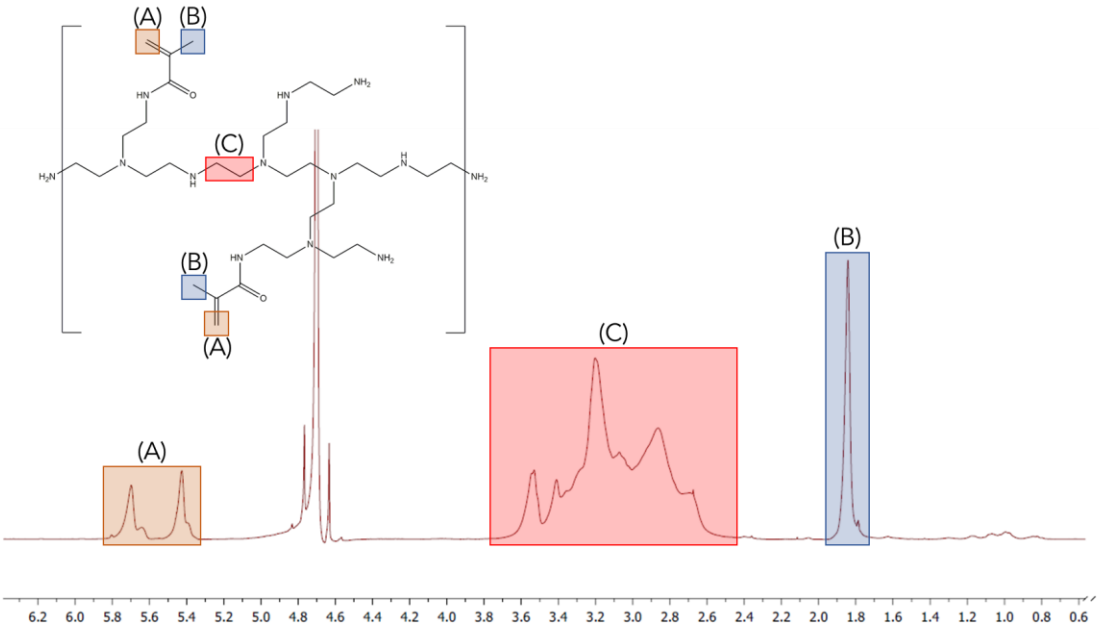

Figure 286. ^{1}H NMR spectra of PEIm. (A) These peaks characteristics of methyl groups in methacrylated moieties were observed at approximately 5.4 and 5.8 ppm. These peaks were not present in the unmodified PEI. The peak (B) located at approximately 1.8 and 2.1 ppm respectively, are the methyl group signals. (C) is the total ^{1}H in the ethylene backbone.

To determine PEI degree of substitution peak B and C of Figure 26 were integrated and multiplied by the number of protons present in the integration window. The degree of substitution was calculated according to the following formula.[26]

$$\text{DS}\ (\%) = \frac{(\text{B}) * 4}{(\text{C}) * 3}$$

The methacrylate modified PEI had a 19% degree of substitution. It is noteworthy to emphasize that the large peaks (C) observed between δ=2.4 ppm and δ=3.8 ppm are attributed to the high abundance of primary, secondary and tertiary amines that affect the overall resolution, this is also observed in other literature reports.[26]

In addition, PEIm was also characterized by using ATR-FTIR spectroscopy as shown in Figure 27.

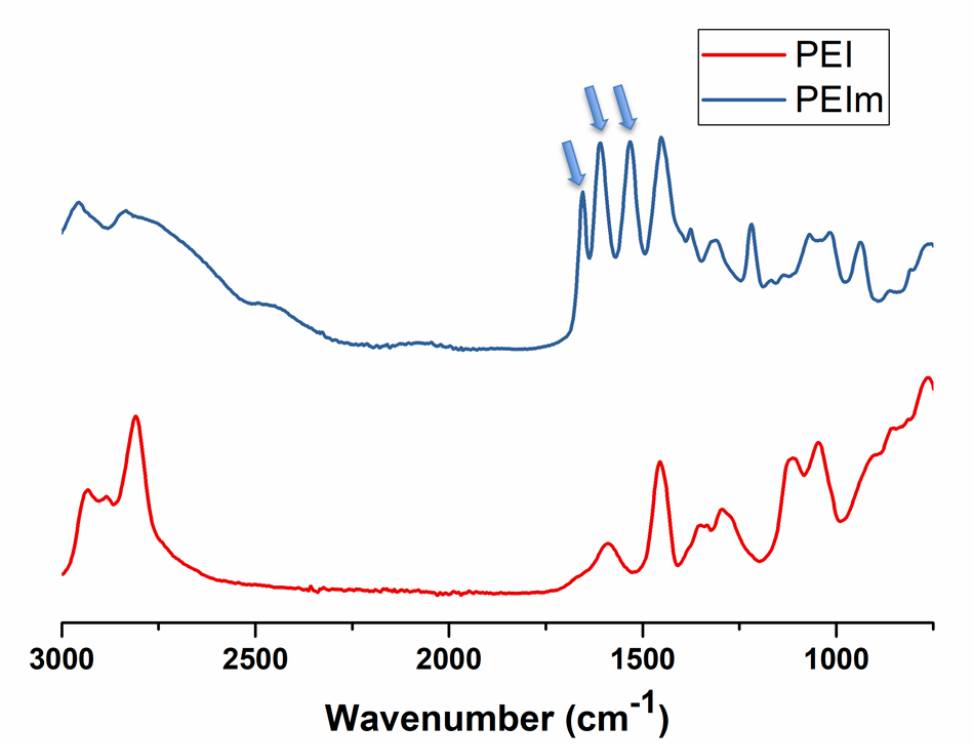

Figure 297. FTIR-ATR Absorbance spectra of PEI and modified PEIm. Blue arrow indicate the most important peaks for methacrylation confirmation.

ATR-FTIR spectroscopy demonstrated the existence of new peaks at ~1652 and 1615 cm^{-1} which can be assigned to the C=O bond and also 1542 cm^{-1} which is related to the C−N bond.[26] These results further verify the successful functionalization of PEI polymeric backbone with methacrylate groups.

3.4. Hyaluronic acid methacrylate synthesis

Hyaluronic acid consists of a repeating unit of D-Glucuronic acid and N-acetyl-D-glucosamine that gives its biodegradable and biocompatible properties. Herein, we modified HA with the methacrylate group through a reaction with glycidyl methacrylate, as reported in the literature [28], to obtain methacrylated hyaluronic acid. The ^{1}H NMR spectra (Figure 28) and FTIR-ATR spectra (Figure 29) are shown and allowed the confirmation of a successful modification.

In the ^{1}H NMR spectrum of methacrylated hyaluronic acid, two new peaks with a chemical shift of δ=5.8 and δ=6.2 ppm were obtained. These peaks are characteristic of methacrylate vinyl groups (Figure 28, (A))[29].

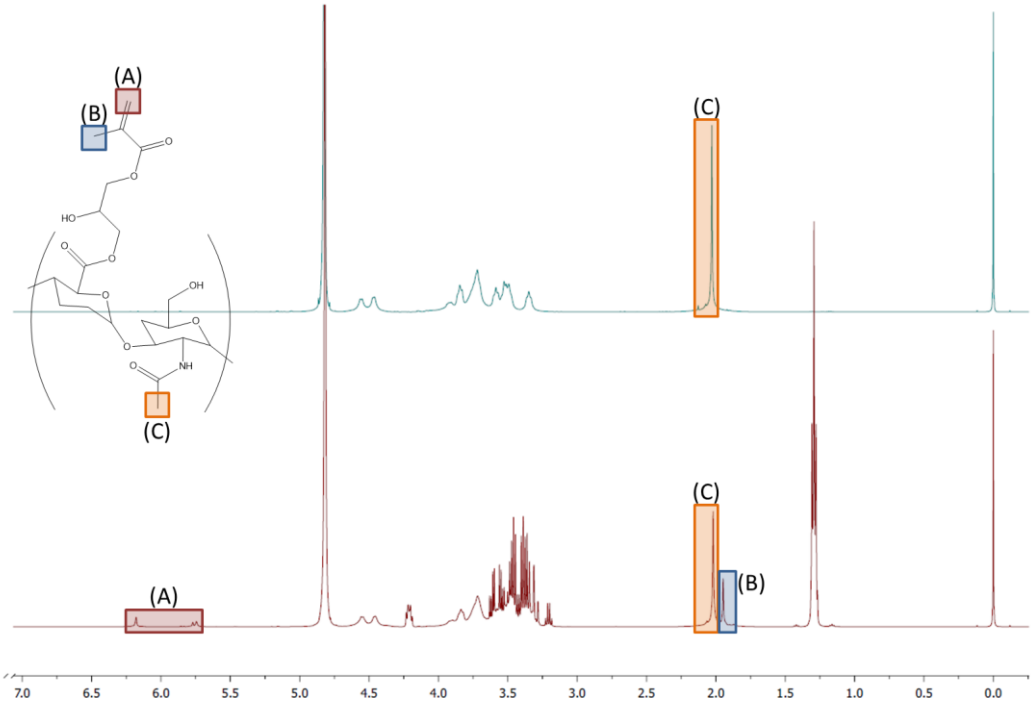

Figure 30. ^{1}H NMR spectra of HAm. (A) These peaks characteristics of methyl groups in methacrylated moieties were observed at approximately δ=5.8 and δ=6.2 ppm. These peaks were not present in the unmodified HA. Also, the peaks B and C located at approximately 1.8 and 2.1 ppm respectively, are the methyl group signals.

To determine the degreed of methacrylate substitution in HA modified polymeric backbone various protons were integrated, B and C in Figure 28.[28] The modified HA had a 35% degree of substitution, indicating that a significant amount of HA D-Glucuronic acid monomers are modified with photo-crosslinkable groups. It is noteworthy to emphasize that

the multiplicity of peaks observed between δ= 3.0 ppm and δ= 3.8 ppm are attributed to the high degree of HA methacrylation as also observed in other recent reports.[28]

In addition, HAm was also evaluated by using FTIR-ATR spectroscopy as shown in Figure 29.

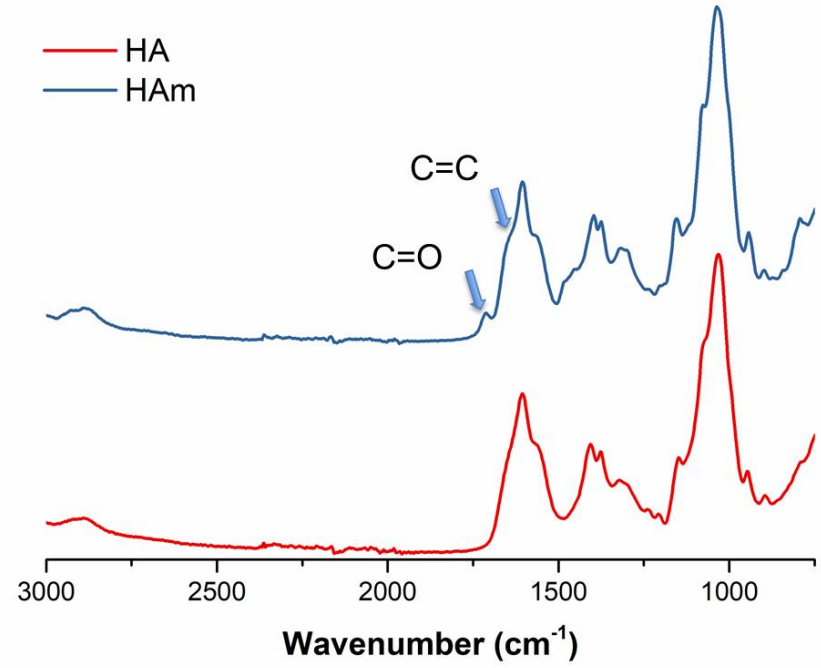

Figure 31. FTIR-ATR absorbance spectra of HA and modified HAm.

FTIR-ATR spectroscopy demonstrated the existence of a new peak at ~1730 cm^{-1} which can be assigned to the C=O bond, and also the existence of a second new peak at 1643 cm^{-1} that is assigned to the C=C bond (Figure 29). These results further verify the successful functionalization of HA polymeric backbone with methacrylate groups.

3.5. Synthesis of PLGA-PEIm NPs via nanoprecipitation

The production of PLGA-PEIm NPs was performed by using the optimal nanoprecipitation conditions as those used for non-methacrylated PLGA-PEI nanoparticles. DLS obtained result indicate the formation of particles with an hydrodynamic diameter of 229.7 nm, PDI~ 0.034 and a surface charge, ζ-potential, of + 12.7 mV. To study the morphology of PLGA-PEIm NPs was characterized by STEM to reduce degradation which result from higher voltages of the TEM equipment (~100 kV). The obtained STEM micrographs of PLGA-PEI NPs where obtained at 20 kV at an NP concentration of 2 mg/mL. Both results can be shown in Figure 30.

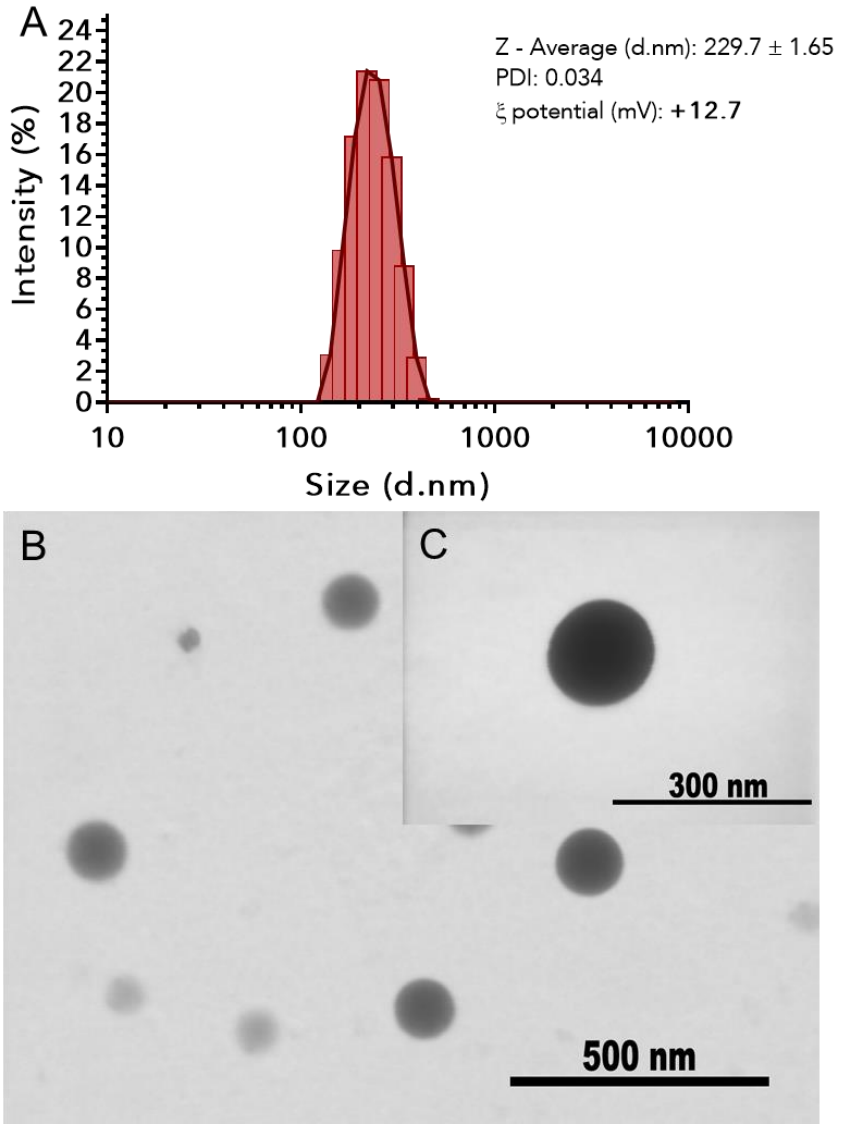

Figure 32. (A) Physicochemical characterization of PLGA-PEIm NPs via DLS analysis. Each measurement was performed in triplicate and includes at least three different replicates (n=3). Morphological analysis through STEM at 20 kV. (B) PLGA-PEI NP (80X) and (C) PLGA-PEI NP (200X).

PLGA is very desired material as it can be processed into any shape and size required and its versatility and easily tunable is proved again in this NP synthesized.[30] PEIm on in contrast to pristine PEI has less amine density and accessible primary amines as some of them are captured by methacrylated groups.[31] This is reflected on the overall surface charge of PLGA-PEIm nanoparticles. This decreased surface charge can be beneficial in the context of a reduced cytotoxicity[32] and the methacrylation provides a new route for U.V. mediated colloidal gels assembly as a double network.

3.6. Synthesis of Zein-HAm NPs via nanoprecipitation

To produce Zein-HAm NPs the protocol developed was adapted from two previously developed works Hae-Yong Seok et al., 2018 and Mary C Regier et al. 2012.[33,34] As followed by previous work the optimal pH to process the particles after nanoprecipitation is pH=8. The synthesized NPs had a hydrodynamic diameter of 155.9 nm, size distribution (PdI) equal to 0.128 and a surface charge, ζ-potential, of -30.4 mV. To study particles morphology, Zein-HAm NPs were characterized by STEM (Figure 31).

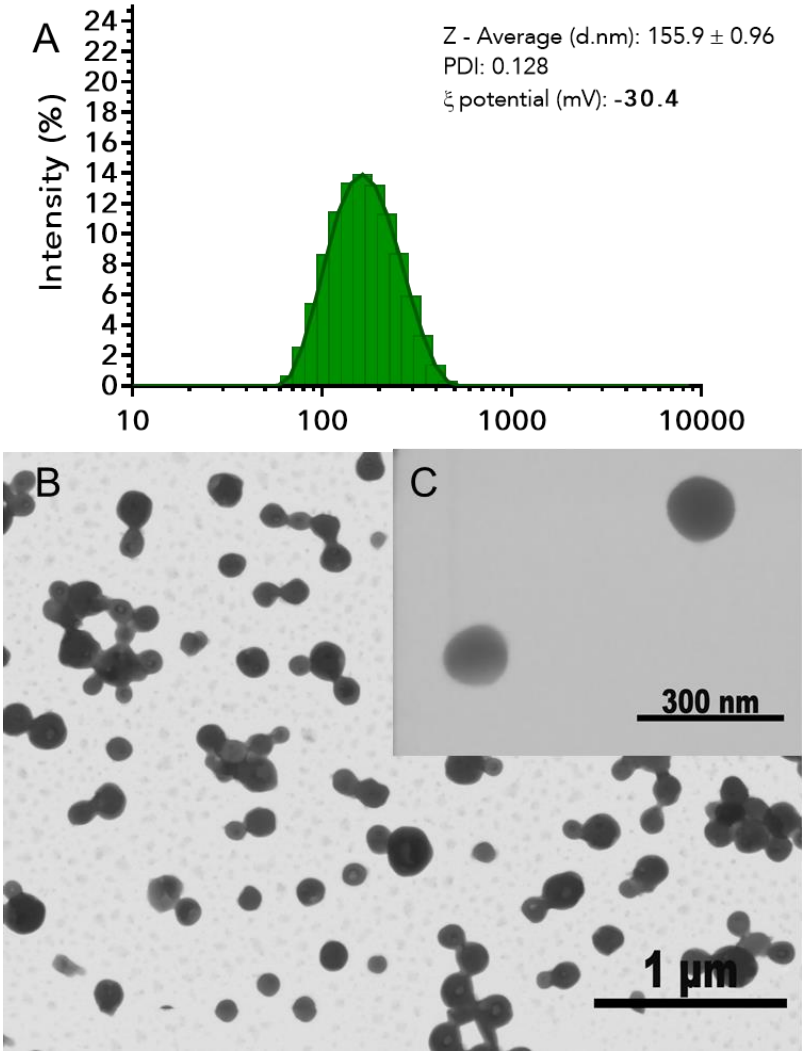

Figure 33. (A) Physicochemical characterization of Zein-HAm NPs via DLS analysis. Each measurement was performed in triplicate and includes at least three different replicates (n=3). Morphological analysis through STEM at 20 kV. (B) Zein-HA NP (30X) and (C) Zein-HA (150X).

3.7. Naringin drug loading efficiency

The Naringin encapsulation efficacy in NPs was determined by UV-VIS analysis of the characteristic flavanone peak at λ= 282 nm in the aqueous solution remain from centrifugated NP formulations. The encapsulation of Naringin in Zein-HAm was performed by dissolving Naringin in Ethanol 80% (w/v) up to a concentration of 1 mg/mL and then mixed with Zein right before nanoprecipitation. To evaluate encapsulation efficacy the final volume of the recovered solution had to be diluted 10-fold. This enables the detection to be in range of the calibration curve (Supplementary Figure S3). The obtain data indicated an encapsulation efficiency (EE) in Zein-HAm NPs of 64 ± 7% (Figure 32). Moreover, as shown by the DLS results particles with encapsulated Naringin showed no significant change in size (Figure 8).

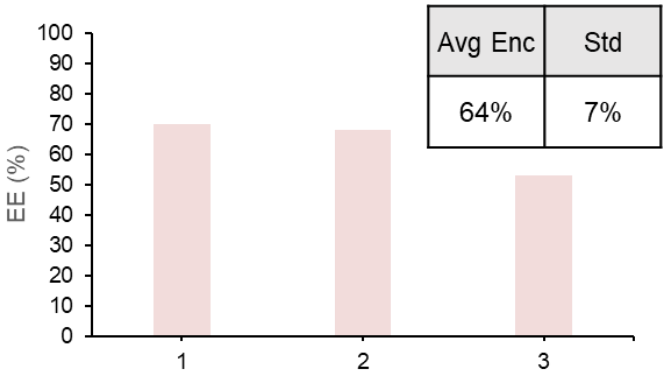

Figure 34. Encapsulation efficiency of naringin in Zein-HAm nanoparticles encapsulation efficiency (n=3).

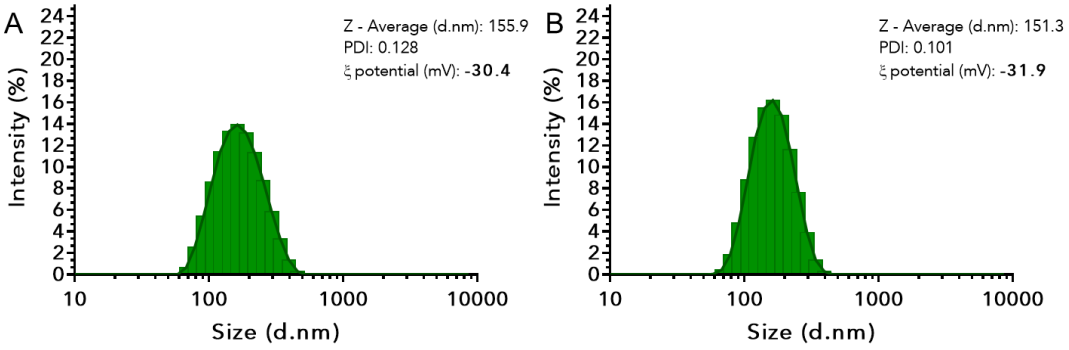

Figure 35. Physicochemical characterization of blank (A) and Naringin-loaded (B) Zein-HAm via DLS analysis. Each measurement was performed in triplicate and includes at least three different replicates (*n*=3).

3.8. Colloidal gel formation

The double network colloidal gel was formulated by taking advantage of both electrostatic complexation between the anionic Zein-HAm NPs and cationic PLGA-PEIm NPs and U.V. mediated photocrosslinking. This dual crosslinking approach allows the obtention that are self-assembled initially by electrostatic interactions of the oppositely charged particles and that can then be *in situ* photocroslinkable and fixed as a stiffer structure. This approach surpasses the current mechanical limitations of electrostatic self-assembled colloidal gels and offers the possibility to produce on site a long-term drug depot device. Moreover, this strategy still allows to take advantage of single network colloidal hydrogels moldability, injectability and fit to shape properties.

Interestingly the use of photocroslinkable moieties also allows the additional formation of colloidal gels comprised by only one nanoparticle type (Zein-HAm NPs or PLGA-PEIm NPs), such is highly advantageous as one could postulate the *in situ* injection of single-type nanoparticle suspensions, followed by photoinduced crosslink to fix the particles in the desired site.

Hence taking this into consideration the colloidal gels were classified as A (Zein-HAm NPs), B (PLGA-PEIm NPs) or AB (Zein-HAm and PLGA-PEIm NPs) from herein forward. The UV-mediated double network colloidal gels formed in PDMS molds are presented in Figure 34.

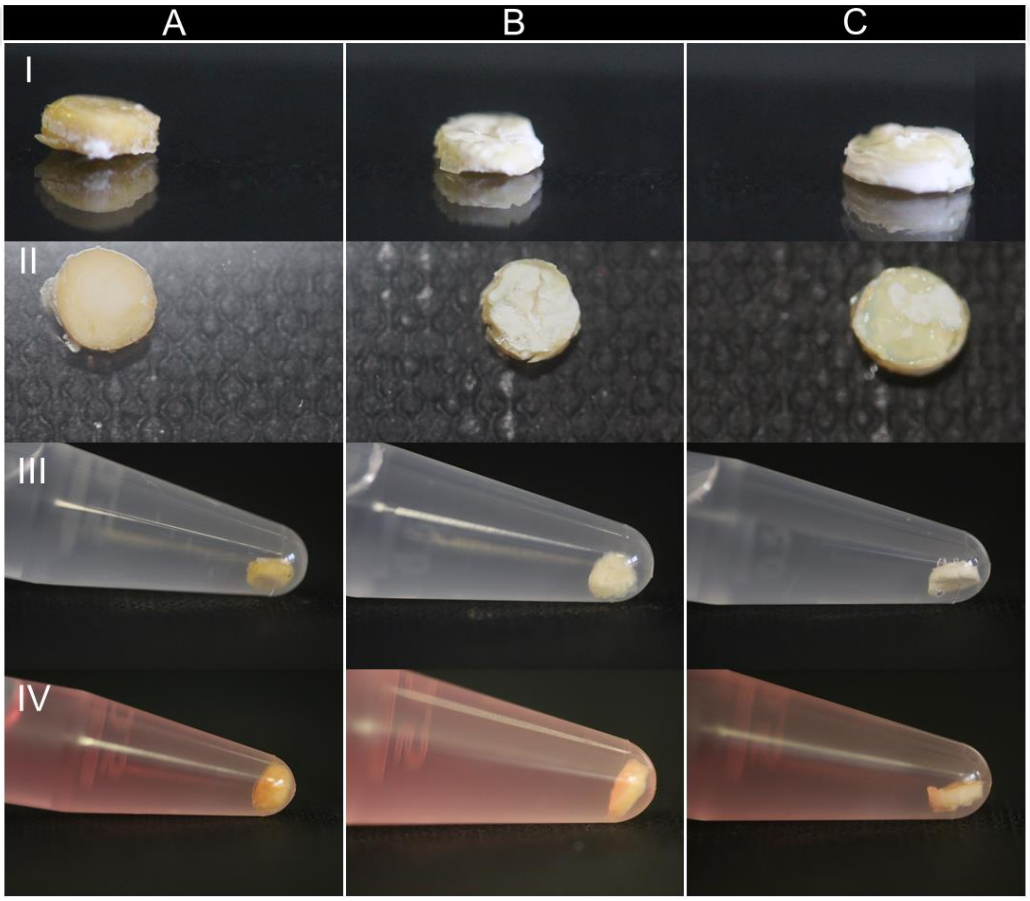

Figure 36. Freshly made colloidal gels from a PDMS mold with a 3.5 mm punch. A column is colloidal gel type A. B column is colloidal gel type AB and C column is colloidal gel type B. Lines I and II are the images of the colloidal gel after coming out of a PDMS mold. III line are the colloidal gels in PBS medium. IV line are colloidal gels in culture medium.

As it can been seen colloidal gels are highly stable in different conditions and retain the disk shape of their mold indicating not only that they retain moldability properties by also showing that the overall structure remains stable enough for manual handling. Interestingly these characteristics were observed for both A, B and AB double network gels.

Another important aspect of the double network hydrogels is the assurance that the electrostatic interactions occur between oppositely charged particles. Hence, to further confirm the homogeneous dispersion of the different NPs in the colloidal matrix PLGA-PEIm NPs were labelled with DiD and Zein-HAm NPs were labelled with DiO and the self-assembled colloidal gels were visualized by widefield fluorescence microscopy.

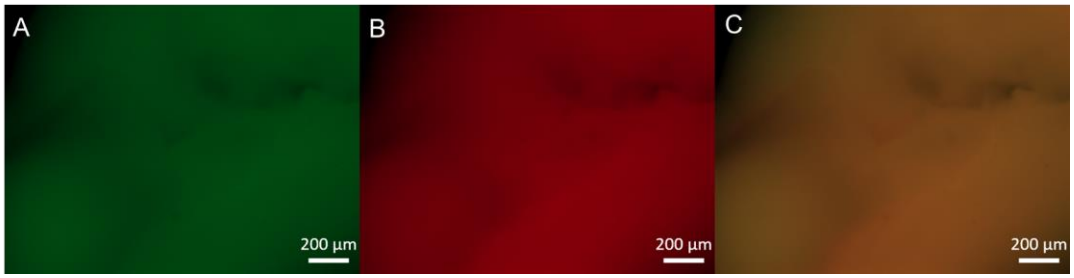

Figure 37. Widefield fluorescence microscopy of colloidal gels with Did and DiO encapsulate in nanoparticles. (A) Microscope image of Zein-HAm NPs with DiO marker in gel. (B) Microscope image PLGA-PEIm NPs with DiD marker in gel. (C) Microscope image of both DiD and DiO, this shown a near complete overlap indicating an interconnecting network between the nanoparticles.

As fluorescence microscopy images demonstrate the particles were dispersed homogeneously throughout the whole gel, indicating a successful mixing between the two oppositely charged nanoparticle types (e.g., Zein-HAm NPs and PLGA-PEIm NPs).

Furthermore, the particle dispersion in the colloidal gel double network and non-irradiated single networks.

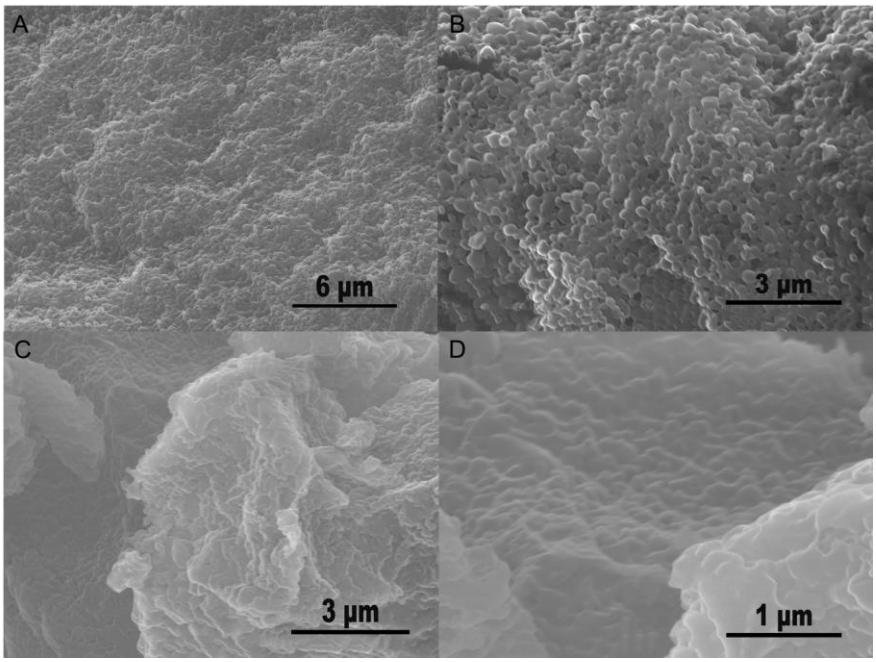

Figure 38. Morphological analysis of colloidal gel through SEM at 15 kV, A (4.5x), B (10x), C (10x) and D (30x). A and B represent colloidal gels after been irradiated with UV light. A and D represent colloidal gels that were not irradiated with UV light.

The network structure of the colloidal gel with the irradiated UV light display a more bulk rough surface which may indicate a higher mechanical stability.[17]

3.9. Release profile of Naringin from Gel-Nar

Different factors influence drug release kinetics, the polymeric matrix and composition of the nanocarrier, its structure and biodegradation kinetics, but also the drug solubility, stability and interaction with the polymeric matrix of the nanocarrier.[37] In the naringin case, the flavonoid has a amphiphilic structure and high stability for a flavone, for instance in comparison with Quercetin. The release medium was comprised by PBS (pH 7.4) containing 0.5% Tween 20 to avoid precipitation of Naringin and assure sink conditions.[38].

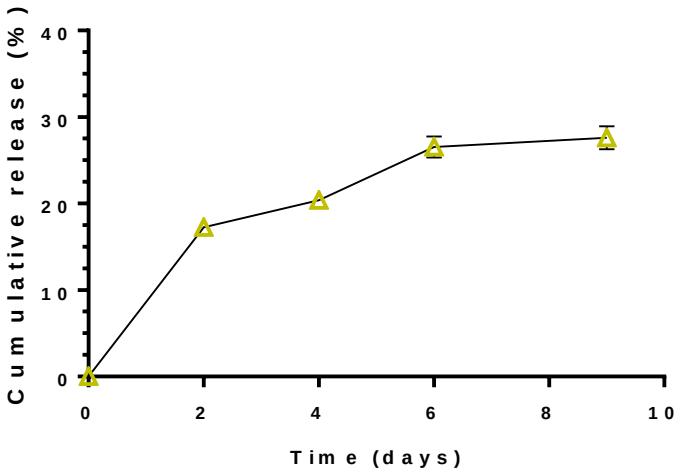

Figure 39. Cumulative release profile of Naringin from colloidal gel in PBS at pH 7.4 containing 0.5% (w/v Tween 20). Data is presented as mean ± s.d. (*n*=2).

The obtained results in Figure 37 are affected by Irgacure presence since Irgacure as its absorbance peak very close to the peak of Naringin and as such influences the reading via UV-vis. Irgacure spectrum in (Supplementary Figure S4).

As such, the only method that could be used to seemingly determine the release profile of the double network colloidal gel was to encapsulate a model hydrophobic dye like DiO and compare its release from the single network and double network in the same conditions (Figure 38).

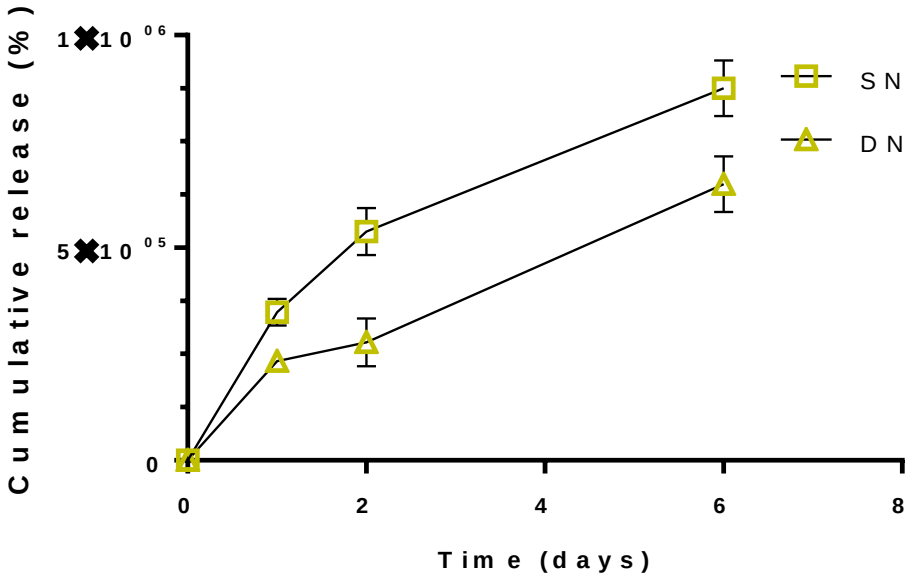

Figure 40. Cumulative release profile of DiO from single network and double colloidal gel in PBS at pH 7.4 containing 0.5% (w/v Tween 20). Data is presented as mean ± s.d. (*n*=3).

These results shown that the double network has a slower release profile than the single network colloidal gel, such is an important finding considering the envisioned future use of these systems as long-term drug depots.

The use of the colloidal gels in a pellet was to mimic its action *in vivo* and present a release profile from the perspective of a focal drug depot.[39]It is hypothesized that the secondary crosslinking creates a more compact colloidal gel which in turn hinders drug diffusion through the colloidal gel matrix.

3.10. Water content

water content was determined for double network colloidal gels as shown in Figure 34.[36] This result demonstrated that the colloidal gel has approximately 50% (w/v) of particles to water, which is almost a 3-fold increase in particle concentration to other referenced works[41], and is quite similar to that obtained for the single network self-assembled colloidal gels.

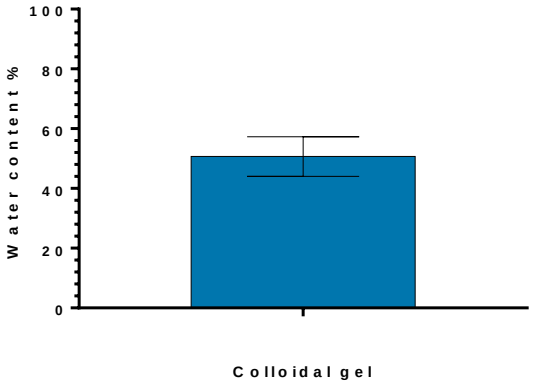

Figure 41. Water content graph represented as the ratio between the freeze-dry colloidal gel to its hydrated form after centrifugation.

3.11. Swelling

The swelling profile of double network hydrogels was determined immediately after UV-mediated crosslinking. This is an important property since swelling can lead to a rapid disruption of macrostructures.[42]

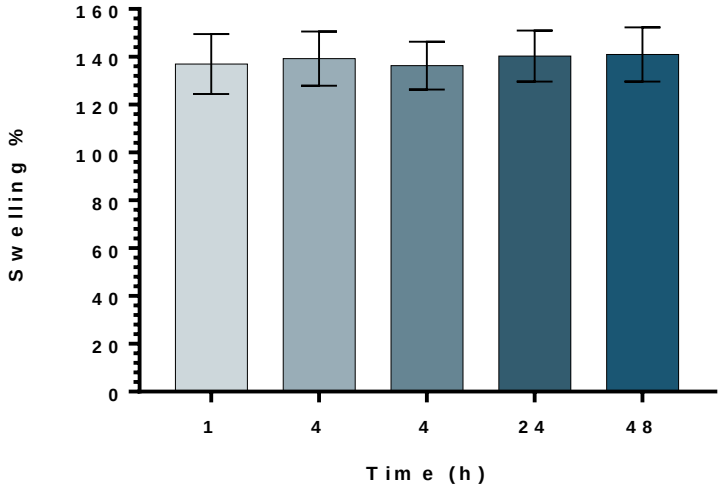

Figure 42. Swelling analysis of double network colloidal gel represented as the ratio between the hydrated colloidal gel at the time point to the freeze-dried colloidal gel. Data is presented as mean ± s.d., (n=4).

In the UV mediated assembly, the swelling of the colloidal gel occurs for a longer period of time. However, the water uptake was significantly less in comparison to electrostatically assembled colloidal gels.

3.12. Mass loss

Mass loss in biomaterials is defined by the loss of material to the medium, in case of colloidal gels is the loss of nanoparticles since the nanoparticle itself is expected to have long bulk degradation kinetics (several months). As the data in Figure 41 demonstrates.[43] that no significant mass loss occurs up to 14 days, indicating the advantageous inclusion of UV mediated photocrosslinking.

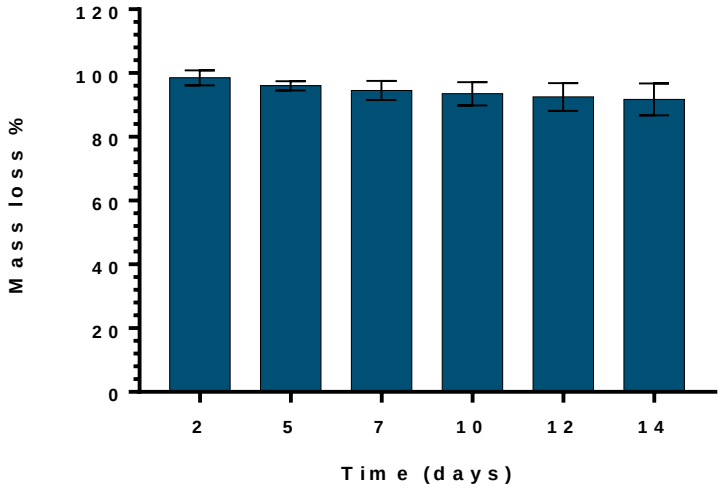

Figure 43. Mass loss graph of the colloidal gel represented as the ratio between the hydrated colloidal gel at the time point to time zero fully hydrated colloidal gel.

3.12.1. Cytotoxicity assay

An ideal colloidal gel does not exert a significant toxic effect upon contact with cells or tissues. The toxicity of the colloidal gel with and without naringin was therefore evaluated in order to determine the feasibility of this system to be used as a focal drug delivery depot in the context of various biomedical applications.

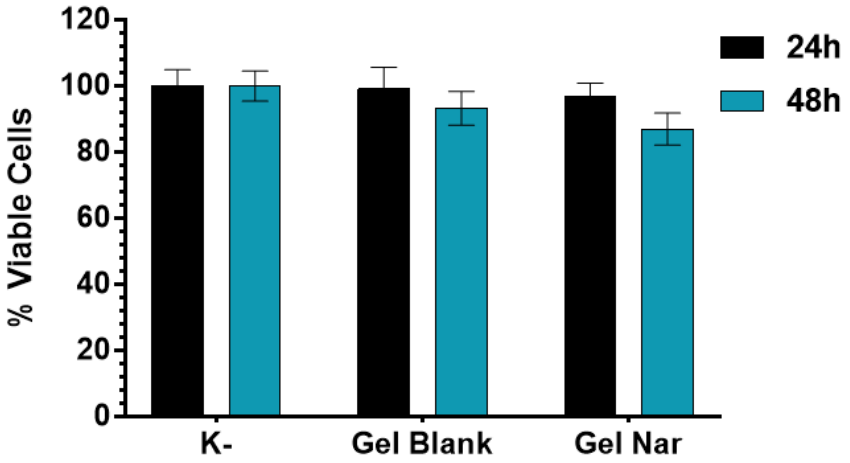

Figure 44. Characterization of the basal medium negative cytotoxicity (K-) control accounts for the 100% viability, the effect of colloidal gel and naringin effect on Gel-Nar were evaluated. Data is presented as mean ± s.d. (n=5).

The results showed that neither blank or drug loaded colloidal gels do not significantly affect cell viability along time.

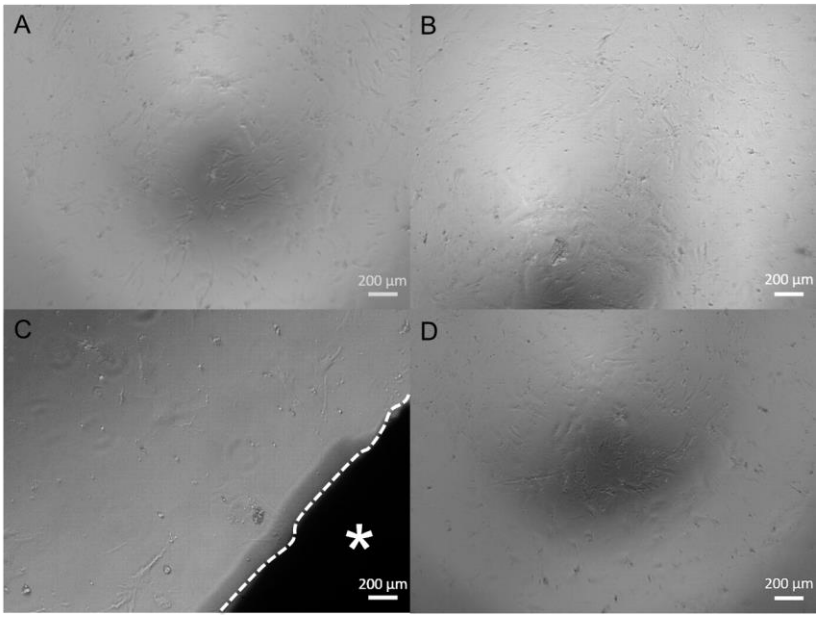

Figure 45. ASCs cell were incubated in a 48 well plate in (A) basal medium, (B) OM as osteogenic control (C) OM in the presence of Gel-Nar* (D) OM with on dose of free naringin.

Moreover, this is corroborated by the optical contrast micrographs which that demonstrate colloidal gels do not affect human adipose derived stem cells (ASCs) morphology along time.

3.10.2 Naringin-induced Stimulation of ALP Activity

Alkaline phosphatase (ALP) is a crucial effector protein is responsible for providing inorganic phosphate and coordinating bone metabolism towards the mineralization of the extracellular matrix.[44] And is, as such, a widely recognized early osteogenesis marker of which plays an important role in bone mineralization.[45]

Typically, for these assays stem cells were cultured in specific osteoinductive media in order to induce osteogenesis. Regarding the osteogenic potential of free Naringin, different literature reports indicate different choices for the osteogenic inductive medium.[46,47,48,49] Herein, we followed the previously implemented protocol the evaluation of Naringin effect on the osteogenic differentiation of ASCs.[50]

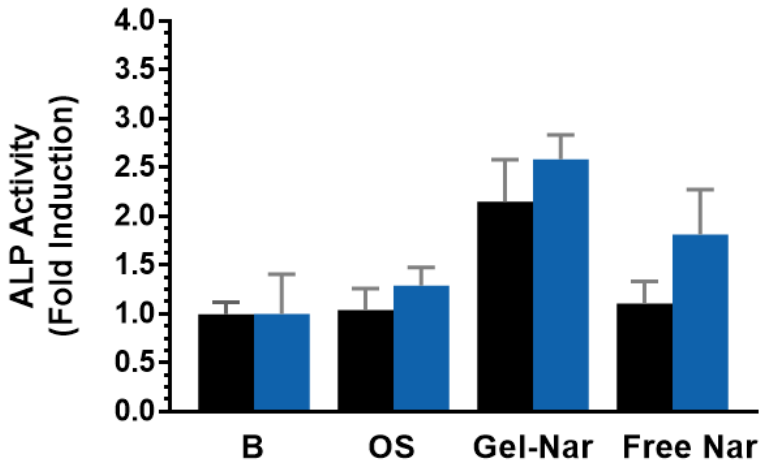

Figure 46. ALP activity of ASCs over 7 and 14 days in BM, OM, Gel-Nar and single dose free naringin, expressed in nmol p-nitrophenol normalized to DNA content. Data represented in mean ± s.d. (n=5).

These results show an increase in ASCs ALP activity along time after incubation in OM control group and a more pronounced effect when Gel-Nar was inserted in culture. The ALP activity is the highest at the final time point of the experiment, *i.e.*, 14 days of incubation. These results might suggest that the continuously release of Naringin from the colloidal gel promotes a constant inflow to the medium of naringin, which does not happen in the other conditions when exchanging the osteogenic medium with a renewed OM.

4. Conclusions

In summary, this study introduced a modified nanoprecipitation method that enabled a one-step preparation of nanosized colloids with a simultaneous outer coating containing homogeneous polymeric layers. The nanoparticles developed showed high monodispersity and suitable physicochemical properties. The first electrostatically driven network acts as a flexible template that enables shaping and molding to fill complex defect sites or inclusion within sophisticated tissue engineering platforms. While PLGA-PEIm and Zein-HAm served efficiently as a Naringin carrier as well as with the pendant methacrylic groups in outer polymeric brushes. Also, the mechanical properties offered by the different method in fabrication compared to other single-network colloidal gels grants a more cohesive nature and facilitates the proximity of the pendant methacrylic groups. The bulk structure of the gel offered a strong platform but with moldable capabilities up until the UV crosslinking is done. It is important to emphasize that additional rheological and mechanical tests should be performed for evaluating the overall properties of the novel double network colloidal gel.

The double network colloidal gel did not pose any toxicity to ASCs. The resulting colloidal gel combines the drug delivery systems of nanocarriers and extends their functionality from nano to a macrostructure with a cohesive network that has shown long term release and the possibility to be used as an *in situ* drug delivery depot.

5. References

1. Bianchi, E., Blaak, R. & Likos, C. N. Patchy colloids: state of the art and perspectives. *Phys. Chem. Chem. Phys.* **13,** 6397 (2011).

2. Patrick Royall, C., Williams, S. R., Ohtsuka, T. & Tanaka, H. Direct observation of a local structural mechanism for dynamic arrest. *Nat. Mater.* **7,** 556–561 (2008).

3. Kohl, M., Capellmann, R. F., Laurati, M., Egelhaaf, S. U. & Schmiedeberg, M. Directed percolation identified as equilibrium pre-transition towards non-equilibrium arrested gel states. *Nat. Commun.* **7,** 11817 (2016).

4. Moore, T. L. *et al.* Nanoparticle colloidal stability in cell culture media and impact on cellular interactions. *Chem. Soc. Rev.* **44,** 6287–6305 (2015).

5. Nel, A. E. *et al.* Understanding biophysicochemical interactions at the nano–bio interface. *Nat. Mater.* **8,** 543–557 (2009).

6. Yin, Y. & Xia, Y. Self-assembly of monodispersed spherical colloids into complex aggregates with well-defined sizes, shapes, and structures. *Adv. Mater.* **13,** 267–271 (2001).

7. Kinnear, C., Moore, T. L., Rodriguez-Lorenzo, L., Rothen-Rutishauser, B. & Petri-Fink, A. Form Follows Function: Nanoparticle Shape and Its Implications for Nanomedicine. *Chem. Rev.* **117,** 11476–11521 (2017).

8. Hotze, E. M., Phenrat, T. & Lowry, G. V. Nanoparticle Aggregation: Challenges to Understanding Transport and Reactivity in the Environment. *J. Environ. Qual.* **39,** 1909 (2010).

9. Gado, E. Del *et al.* Colloidal Gelation. in *Fluids, Colloids and Soft Materials: An Introduction to Soft Matter Physics* (eds. Fernandez-Nieves, A. & Puertas, A. M.) 279–290 (Wiley, 2016). doi:10.1002/9781119220510

10. Diba, M. *et al.* Nanostructured raspberry-like gelatin microspheres for local delivery of multiple biomolecules. *Acta Biomater.* **58,** 67–79 (2017).

11. Tanaka, H. & Araki, T. Simulation Method of Colloidal Suspensions with Hydrodynamic Interactions: Fluid Particle Dynamics. *Phys. Rev. Lett.* **85,** 1338–1341 (2000).

12. Diba, M. *et al.* Self-Healing Biomaterials: From Molecular Concepts to Clinical Applications. *Adv. Mater. Interfaces* **5,** 1800118 (2018).

13. Diba, M., Wang, H., Kodger, T. E., Parsa, S. & Leeuwenburgh, S. C. G. Highly Elastic and Self-Healing Composite Colloidal Gels. *Adv. Mater.* **29,** (2017).

14. Montgomery, M. *et al.* Flexible shape-memory scaffold for minimally invasive delivery of functional tissues. *Nat. Mater.* **16,** 1038–1046 (2017).

15. Kowalski, P. S., Bhattacharya, C., Afewerki, S. & Langer, R. Smart Biomaterials: Recent Advances and Future Directions. *ACS Biomater. Sci. Eng.* **4,** 3809–3817 (2018).

16. Wang, Q., Jamal, S., Detamore, M. S. & Berkland, C. PLGA-chitosan/PLGA-alginate nanoparticle blends as biodegradable colloidal gels for seeding human umbilical cord mesenchymal stem cells. *J. Biomed. Mater. Res. - Part A* **96 A,** 520–527 (2011).

17. Wang, Q., Wang, L., Detamore, M. S. & Berkland, C. Biodegradable colloidal gels as moldable tissue engineering scaffolds. *Adv. Mater.* **20,** 236–239 (2008).

18. Diba, M. *et al.* Composite Colloidal Gels Made of Bisphosphonate-Functionalized Gelatin and Bioactive Glass Particles for Regeneration of Osteoporotic Bone Defects. *Adv. Funct. Mater.* **27,** 1703438 (2017).

19. Wang, H. *et al.* Comparison of micro- vs. nanostructured colloidal gelatin gels for sustained delivery of osteogenic proteins: Bone morphogenetic protein-2 and alkaline phosphatase. *Biomaterials* **33,** 8695–8703 (2012).

20. Wang, H. *et al.* Combined delivery of BMP-2 and bFGF from nanostructured colloidal gelatin gels and its effect on bone regeneration in vivo. *J. Control. Release* **166,** 172–181 (2013).

21. Wang, H. *et al.* Development of injectable organic/inorganic colloidal composite gels made of self-assembling gelatin nanospheres and calcium phosphate nanocrystals. *Acta Biomater.* **10,** 508–519 (2014).

22. Yan, C. *et al.* Injectable solid hydrogel: mechanism of shear-thinning and immediate recovery of injectable β-hairpin peptide hydrogels. *Soft Matter* **6,** 5143 (2010).

23. Geraghty, R. J. *et al.* Guidelines for the use of cell lines in biomedical research. *Br. J. Cancer* **111,** 1021–1046 (2014).

24. Rampersad, S. N. Multiple applications of alamar blue as an indicator of metabolic function and cellular health in cell viability bioassays. *Sensors (Switzerland)* **12,** 12347–12360 (2012).

25. Holycross, D. R. & Chai, M. Polymers. 4–10 (2013).

26. Paciello, A. & Santonicola, M. G. Supramolecular polycationic hydrogels with high swelling capacity prepared by partial methacrylation of polyethyleneimine. *RSC Adv.* **5,** 88866–88875 (2015).

27. Zhang, Q. F. *et al.* Amino acid-modified polyethylenimines with enhanced gene delivery efficiency and biocompatibility. *Polymers (Basel).* **7,** 2316–2331 (2015).

28. A, S. *et al.* A facile one-pot synthesis of acrylated hyaluronic acid. *Chem. Commun.* **54,** 1081–1084 (2018).

29. Weeks, A. *et al.* Photocrosslinkable hyaluronic acid as an internal wetting agent in model conventional and silicone hydrogel contact lenses. *J. Biomed. Mater. Res.* **100A,** 1972–1982 (2012).

30. Ding, D. & Zhu, Q. Recent advances of PLGA micro/nanoparticles for the delivery of biomacromolecular therapeutics. *Mater. Sci. Eng. C* 0–1 (2018). doi:10.1016/j.msec.2017.12.036

31. Ma, Y. *et al.* Polyethylenimine nanofibrous adsorbent for highly effective removal of anionic dyes from aqueous solution. *Sci. China Mater.* **59,** 38–50 (2016).

32. García, M. C. & Cuggino, J. C. *Stimulus-responsive nanogels for drug delivery*. *Stimuli Responsive Polymeric Nanocarriers for Drug Delivery Applications, Volume 1* (Elsevier Ltd., 2018). doi:10.1016/B978-0-08-101997-9.00016-3

33. Seok, H. *et al.* CD44 targeting biocompatible and biodegradable hyaluronic acid cross-linked zein nanogels for curcumin delivery to cancer cells: In vitro and in vivo evaluation. *J. Control. Release* **280,** 20–30 (2018).

34. Regier, M. C., Taylor, J. D., Borcyk, T., Yang, Y. & Pannier, A. K. Fabrication and characterization of DNA-loaded zein nanospheres. *J. Nanobiotechnology* **10,** 1 (2012).

35. Malekzad, H. *et al.* Plant protein-based hydrophobic fine and ultrafine carrier particles in drug delivery systems. *Crit. Rev. Biotechnol.* **38,** 47–67 (2018).

36. Roux, R., Ladavière, C., Montembault, A. & Delair, T. Particle assemblies: Toward new tools for regenerative medicine. *Mater. Sci. Eng. C* **33,** 997–1007 (2013).

37. Fu, Y. & Kao, W. J. Drug release kinetics and transport mechanisms of non-degradable and degradable polymeric delivery systems. *Expert Opin. Drug Deliv.* **7,** 429–444 (2010).

38. Nguyen, T. T. & Jeong, J. H. Development of a single-jet electrospray method for producing quercetin-loaded poly (lactic-co-glycolic acid) microspheres with prolonged-release patterns. *J. Drug Deliv. Sci. Technol.* **47,** 268–274 (2018).

39. Siepmann, J. & Peppas, N. A. Modeling of drug release from delivery systems based on hydroxypropyl methylcellulose (HPMC). *Adv. Drug Deliv. Rev.* **64,** 163–174 (2012).

40. Zia, R. N., Landrum, B. J. & Russel, W. B. A micro-mechanical study of coarsening and rheology of colloidal gels: Cage building, cage hopping, and Smoluchowski's ratchet. *J. Rheol. (N. Y. N. Y).* **58,** 1121–1157 (2014).

41. Wang, Q., Wang, J., Lu, Q., Detamore, M. S. & Berkland, C. Injectable PLGA based colloidal gels for zero-order dexamethasone release in cranial defects. *Biomaterials* **31,** 4980–4986 (2010).

42. Khan, F. & Tanaka, M. Designing smart biomaterials for tissue engineering. *Int. J. Mol. Sci.* **19,** 1–14 (2018).

43. Yang, R. & Liang, H. Dynamic electro-regulation of the stiffness gradient hydrogels. *RSC Adv.* **8,** 6675–6679 (2018).

44. Marom, R., Shur, I., Solomon, R. & Benayahu, D. Characterization of adhesion and differentiation markers of osteogenic marrow stromal cells. *J. Cell. Physiol.* **202,** 41–48 (2005).

45. Granéli, C. *et al.* Novel markers of osteogenic and adipogenic differentiation of human bone marrow stromal cells identified using a quantitative proteomics approach. *Stem Cell Res.* **12,** 153–165 (2014).

46. Liao, H.-T. Osteogenic potential: Comparison between bone marrow and adipose-derived mesenchymal stem cells. *World J. Stem Cells* **6,** 288 (2014).

47. Wall, M. E., Bernacki, S. H. & Loboa, E. G. Effects of Serial Passaging on the Adipogenic and Osteogenic Differentiation Potential of Adipose-Derived Human Mesenchymal Stem Cells. *Tissue Eng.* **13,** 1291–1298 (2007).

48. Kyllönen, L. *et al.* Effects of different serum conditions on osteogenic differentiation of human adipose stem cells in vitro. *Stem Cell Res. Ther.* **4,** 1–15 (2013).

49. Racine, L. *et al.* Time-Controllable Lipophilic-Drug Release System Designed by Loading Lipid Nanoparticles into Polysaccharide Hydrogels. *Macromol. Biosci.* **17,** 1–11 (2017).

50. Lavrador, P., Gaspar, V. M. & Mano, J. F. Bioinstructive Naringin-Loaded Micelles for Guiding Stem Cell Osteodifferentiation. *Adv. Healthc. Mater.* **7,** 1–16 (2018).

6. Annexes

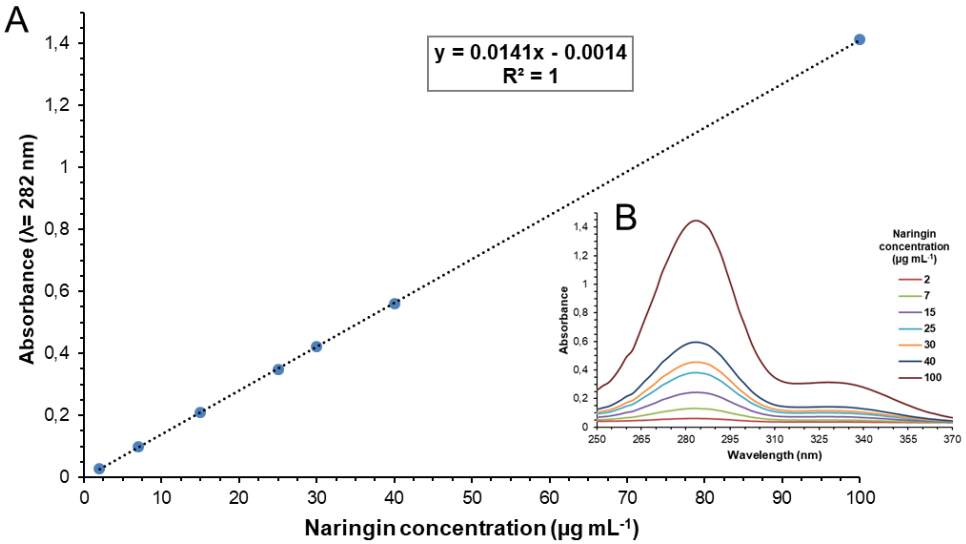

Figure 47. (A) Calibration curve of naringin in H_2O at λ=282 nm. (B) Inset represents the absorbance spectrum of Naringin within a spectral window of 200 to 450 nm.

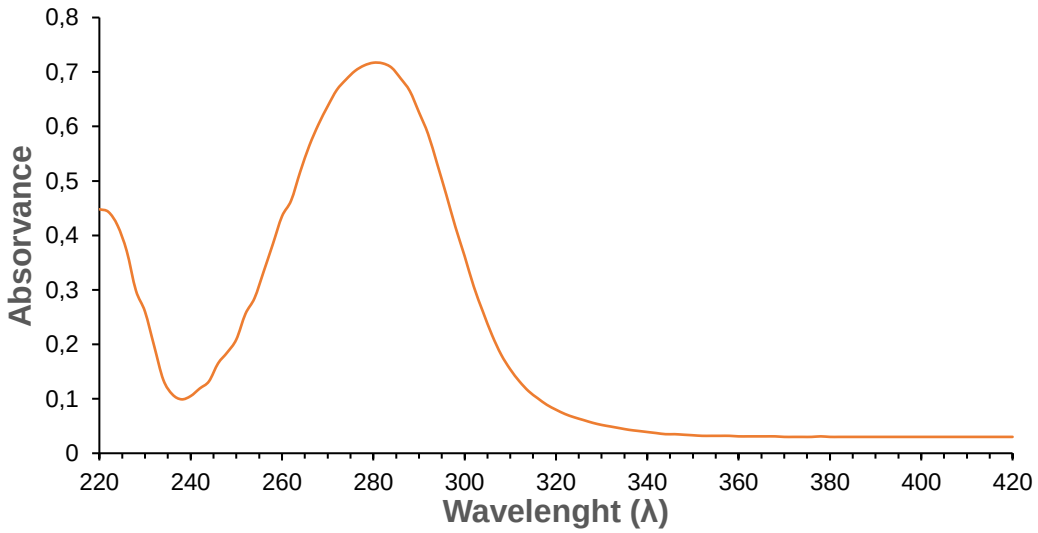

Figure 48. Irgacure Uv-vis detection at 200-fold diluted from stock solution 1% (w/v)

4.General Conclusions and Future perspectives

5. General Conclusions and Future Perspectives

Colloidal gels are remarkable platforms for focal drug delivery. Both anti-inflammatory and tissue engineering applications worked well and cells behaviour was influenced. The PLGA-PEI NPs developed had significant colloid stability in aqueous solutions. Its manipulation is rather easy for a NP as the plasticity did not compromise any handling. Zein-HA NP were on the other side more difficult to handle due to their pH-driven innate aggregation during washing processes, although afterwards these NPs were stable in colloid solutions.

In the first work regarding single network colloidal gels, the obtained gel had promising results throughout the various assays performed. Indeed, quercetin loaded Zein hyaluronic nanoparticles served as efficient nanocarrier systems for drug delivery. The formulated colloidal gel loaded with quercetin, Gel-Q, serves as a long-term drug delivery system, as demonstrated by the *in vitro* release profiles. In the future, however, release of quercetin from the gel should also be evaluated in mildly acidic conditions (pH=6.5), because inflammation sites are typically acidic. Moreover, the cell assays should be further confirmed with additional TNF-α ELISA and LegendPLEX^{TM} immunoassays. In conclusion, the bulk structure of the gel offered a strong platform with moldable capabilities, which opens exciting opportunities for advanced therapeutic applications.

In the second work regarding the double network colloidal gels, the photo-crosslinking mechanism implemented created a completely new platform for therapeutic delivery and biomedical applications. The obtained colloidal gel maintains the appealing moldable capabilities, however after photo-crosslinking it retains the shape, which enables a flexible moldable and fixable platform. While PLGA-PEIm and Zein-HAm NP served as efficient Naringin carriers, while the pendant methacrylic groups in outer polymeric brushes allowed rapid and external network photocrosslinking into a robust and stable platform able to release this bioactive molecule. The bioactive double network gels showed promising osteogenic results compared to free drug. However, cell assays should be further extended to 21 days to fully evaluate the osteogenic potential of the colloidal gel. It is important to emphasize that additional rheological and mechanical tests should be performed for evaluating the overall properties of the novel double network gels. One further study could be the use of PLGA-PEI and PLGA-PEIm NPs as drug depots and explore potential synergetic effects via a dual release platform with independent release profiles and different bioactive molecules.